HONEYCOMB THERMAL SHIELD

USERS MANUAL

SSEC No.76.05.D1

A REPORT

from the space science and engineering center
the university of wisconsin-madison
madison, wisconsin

HONEYCOMB THERMAL SHIELD

USERS MANUAL

Contract Number NAS 5-20068

Prepared by

R. M. Dombroski
Space Science and Engineering Center
The University of Wisconsin
Madison, Wisconsin

for

The NASA/Goddard Space Flight Center
Greenbelt, Maryland

5/31/76

TABLE OF CONTENTS

1.0 Introduction

A Honeycomb Thermal Shield is an economical, simple, and reliable alternative to existing thermal shielding methods for reducing the radiated heat loss from areas which can not allow continuous obstructions in the field of view.

The shield material is simply open-face honeycomb of the type used throughout the aerospace industry for structural panels. The Honeycomb Thermal Shield uses only the core of the honeycomb panel. It has little structural stiffness, but it is transparent through the cells (see Figure 1). It can be located in close proximity to, but conductively decoupled from, the heat source which requires shielding with the axis of the honeycomb cells parallel to the desired view direction. The view field will be clear along the axis of the honeycomb but will be increasingly obscured as the off-normal view angle increases. This angular dependence is a function of the cell height to width ratio.
A source with a narrow field of view will allow a shield with deep cells (large height to width ratio), and will efficiently trap the radiated energy.

The design data and test results referenced in this guide were prepared as part of the Honeycomb Thermal Shield Study which was funded under Contract NAS5-20068 by the NASA Goddard Space Flight Center. The purpose of the guide is to provide design information in a form which can be used to evaluate the Honeycomb Thermal Shield as an alternative to other shielding methods. Details of the mathematical model which were used as a basis for the design curves are described in the February 1975 Honeycomb Thermal Shield Final Report.

2.0 Honeycomb Shield Guidelines and Applications

The Honeycomb Thermal Shield is effective in reducing the radiated energy loss from a heat source to a cold sink. Figure 2 illustrates the modes and direction of heat transfer between the participating thermal elements for two possible shield configurations.

The first configuration requires the shield be conductively isolated from all sinks, and energy transfer between elements 2 and 4 in Figure 2 would be zero. This configuration offers the maximum reduction in heat loss from the system (i.e., minimum transfer to element 2). The energy which the shield radiates to space is supplied by the hot sink, and none is supplied by the frame heat sink.

The second mode requires the shield to be conductively coupled to the frame heat sink. The heat loss from the hot sink is reduced, but at the expense significant energy input from the frame sink. The total heat loss to the cold sink is greater than that for the isolated shield.

Applications of the Honeycomb Thermal Shield thus far have been for low spectral energy, narrow field-of-view x-ray detectors. Sensitivity to low energy x-rays requires an open area, but only along the narrow view field. The size of the honeycomb cell can be selected to be clear within the sensitive zone yet trap most of the radiated energy. Many instruments of this type now being fabricated for spacecraft applications have large apertures which are potential sources of significant heat loss. These detectors also have an inherent sensitivity to thermal gradients, and these gradients are accentuated by the aperture heat loss.

Selection of the conductively isolated or conductively coupled configuration will depend on the dominant system requirement. Where detector gradients must be absolutely minimized, the conductively coupled

configuration is required since the energy loss from the detector is a minimum. A larger heat loss from the shield to the cold sink is sacrificed, though. In addition, a more detailed thermal analysis is required. Where the total heat loss from the combination of detector and spacecraft must be minimized, the conductively isolated configuration is required.

It is important to access the impact of reduced field of view on the instrument due to the influence of the honeycomb shield. Appendix C is offered as an approximation which may allow specification of a range of honeycomb cell sizes.

3.0 Design Guidelines

It is important to keep in mind that the heat transfer through the conductively isolated shield is one-dimensional, whereas the conductively coupled shield is governed by three-dimensional heat transfer. The estimation of energy transfer through the isolated shield is therefore simpler and more reliable.

To determine the heat loss from a Honeycomb Thermal Shield, the following information is required:

1) cell width across flats, (W)
2) cell height, (H)
3) thermal conductivity, (k)
4) wall thickness, (t)
5) emissivity, (ε)
6) temperature of hot sink, (T_1)
7) temperature of cold sink, (T_2)
8) temperature of the honeycomb frame, (T_o) (conductively coupled only)
9) aperture area

Five dimensionless groups govern the performance of the HTS. These parameters, developed in detail in the February 1975 report, are:

1) emissivity, (ε)
2) $(H/W)\sin 60°$, (L)
3) $\frac{H^2\sigma T_1^4}{ktT_o}$, ($N_c$)
4) (T_o/T_1) (conductively coupled only)
5) N, (number of cells), (conductively coupled only)

The first three of the five dimensionless parameters apply only to the conductivity isolated configuration.

The design graphs which follow present the honeycomb efficiency, η, as a function of the dimensionless parameters N_c, L, ε, (To/T_1), and cell position. Efficiency is defined as:

$$\eta_x = 1 - \frac{QRAD(X)}{\sigma A_1 (T_1^4 - T_2^4)}$$

The subscript x, above, refers to either surface 1 (hot sink) or surface 2 (cold sink). The right-hand term in the equation is the ratio of energy lost (or gained) by the surface to the energy lost (or gained) by that surface if no shield were present.

3.1 Conductively Isolated Shield

Figures 6 and 7 illustrate the dependence of efficiency on N_c, L and ε (T_o/T_1 and cell position do not play a role for this configuration). Using the algorithm of Section 3.3, the heat loss from the shield may be determined.

3.2 Conductively Coupled Shield

The design curves of Figures 8 through 16 provide the information required to determine the energy loss for the conductively coupled configuration. The curves are expressed as efficiency, η, versus cell position for specified:

1) Nc
2) L
3) ε
4) T_o/T_1
5) direction of lateral heat flow

Item 5, above, adds two significant complications to the analysis of this configuration because:

1) cell efficiency is a function of distance from the shield perimeter
2) honeycomb is anisotropic, therefore, the efficiency depends on the direction of heat flow.

Figure 3 illustrates an isolated row of cells oriented in the high conductance direction, and Figure 4 illustrates an isolated row in the low conductance direction. Isolated rows of this type are used to simplify the model of the composite shield by defining lines of constant efficiency as noted in Figure 5.

The row can be assumed isolated if the following conditions are satisfied:

1) Adjacent cells along the path are at similar temperatures.
2) The last cell (farthest from the conductive sink) is at the center of the shield.

In order to distinguish between heat lost from the hot sink and heat lost from the frame sink, it is necessary to define two efficiencies:

$$\eta_1 = 1 - \frac{QRAD(1)}{\sigma A_1 (T_1^4 - T_2^4)}$$

$$\eta_2 = 1 - \frac{QRAD(2)}{\sigma A_1 (T_1^4 - T_2^4)}$$

Where η_1 is the efficiency relative to the loss from the hot sink and η_2 is the loss relative to the input to the cold sink.

These relationships may be rewritten to define the net heat transfer of each element:

$$QRAD(1) = (1-\eta_1)\sigma A_1(T_1^4-T_2^4)$$

$$QRAD(2) = (1-\eta_2)\sigma A_1(T_1^4-T_2^4)$$

$$QSINK - QRAD(2) - QRAD(1)$$

The algorithm of Section 3.4 defines a method to determine η_1 and η_2.

3.3 Conductively Isolated Shield Design Algorithm

1) Determine the following parameters:

   a) W, H, k, t, ε

   b) T_1, T_2

   c) area of the honeycomb shield, A_1

2) Calculate L and N_c

   a) $L = \left(\frac{H}{W}\right)\sin 60°$

   b) $N_c = \frac{H^2\sigma T_1^3}{kt}$

3) Find η from Figure 6 or 7 for appropriate N_c, L and ε

4) Calculate the total heat loss:

$$QRAD(1) = QRAD(2) = (1-\eta)\sigma A_1(T_1^4-T_2^4)$$

3.4 Conductively Coupled Shield Design Algorithm

1) Determine the following parameters:

   a) W, H, k, t, ε

   b) T_1, T_2, T_o

   c) dimensions of honeycomb shield

2) Calculate L, N_c, T_o/T_1

a) $L = \left(\frac{H}{W}\right) \sin 60°$

b) $N_c = \frac{H^2 \sigma T_1^4}{ktT}$

3) Calculate the number of cells in an isolated cell row. For a square shield X inches on a side:

$N = \frac{X}{2W}$ for high conductance direction

$N = \frac{X}{2W\sin 60°}$ for low conductance direction

4) Using the information collected is Steps 1 thru 4, find the appropriate design graphs from Figures 8 thru 16. It may be necessary to generate new design curves based on extrapolations of the information presented in these figures. As a minimum, four curves are required: η_1 and η_2 for both the high and low conductance direction.

5) Determine the cell number on the low conductance graph which corresponds to the lowest value of η_1 for the high conductance graph.

6) Complete tables WS-1, WS-2, WS-3, and WS-4 using the relationships given below: The purpose of the tables is to calculate zone-average efficiencies for η_1 and η_2. Four areas are generally sufficient. The highest cell number should be that determined in Step 5.

A) For a square shield X inches on a side:

$D_L = X - 2(R)$ (R and S defined in Tables WS-1 and WS-2)

$D_H = X - 2(S)$

B) A_E = Ellipse Area = $(D_L)(D_H)\frac{\pi}{4}$ (for n = 1 to 3 where n is the area identification number)

C) A_Z = Zone Area = A_E (for n = 1)

$= A_E)_2 - A_E)_1$ (for n = 2

$= A_E)_3 - A_E)_2$ (for n = 3)

= Total Shield Area - A_{E3} for (n = 4)

D) Average Zone Efficiencies (Table WS-1 for η_1 and WS-2 for η_2)

i) Zone 1; η from line 3 of Table

ii) Zone 2; arithmetic average of η from lines 3 and 2

iii) Zone 3; arithmetic average of η from lines 2 and 1

iv) Zone 4; η from line 1 of table

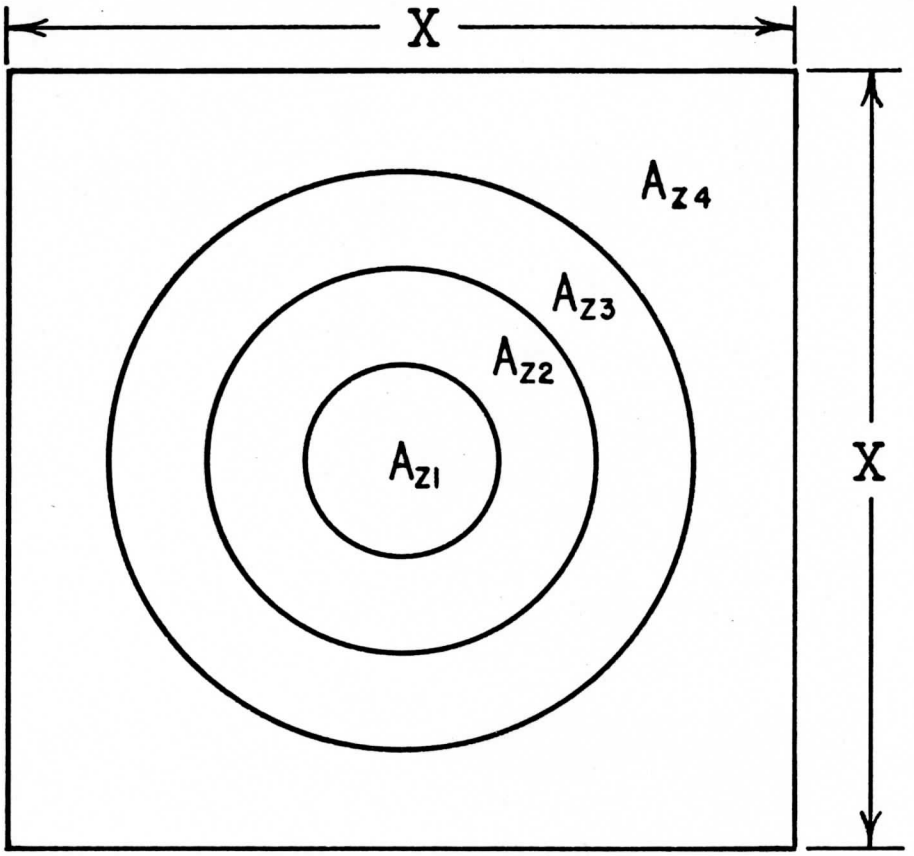

7) Using the average zone efficiencies listed in tables WS-3 and WS-4, calculate the area average efficiencies for η_1 and η_2 :

$$\eta)_{ave} = \frac{\eta)_{zone\ 1}\ A_{Z1} + \eta)_{zone\ 2} A_{Z2} \quad . \ . \ . \ . \ . \ . + \eta)_{zone\ 4} A_{Z3}}{X^2}$$

8) Calculate the heat transfer rates:

$$QRAD(1) = [1-\eta_1)_{ave}]\ \sigma A\ (T_1{}^4-T_2{}^4)$$

$$QRAD(2) = [1-\eta_2)_{ave}]\ \sigma A_1 (T_1{}^4-T_2{}^4)$$

$$QSINK = QRAD(2)-QRAD(1)$$

TABLE WS – 1

LINE NO.	η_1	LOW CONDUCTANCE CELL NO.	LOW CONDUCTANCE DIM. (R)	HIGH CONDUCTANCE CELL NO.	HIGH CONDUCTANCE DIM. (S)
1					
2					
3					
4					

TABLE WS – 2

LINE NO.	η_2	LOW CONDUCTANCE CELL NO.	LOW CONDUCTANCE DIM. (R)	HIGH CONDUCTANCE CELL NO.	HIGH CONDUCTANCE DIM. (S)
1					
2					
3					
4					

TABLE WS – 3 (Based on values in TABLE WS – 1)

AREA ID.	(D_L) ELLIPSE DIA. IN LOW CONDUCTANCE DIRECTION	(D_H) ELLIPSE DIA. IN HIGH CONDUCTANCE DIRECTION	(A_E) ELLIPSE AREA	(A_Z) ZONE AREA	AVERAGE ZONE EFFICIENCY η_1
(1)					
(2)					
(3)					
(4)	– – – –	– – – –	TOTAL SHIELD AREA		

TABLE WS – 4 (Based on values in TABLE WS – 2)

AREA ID.	(D_L) ELLIPSE DIA. IN LOW CONDUCTANCE DIRECTION	(D_H) ELLIPSE DIA. IN HIGH CONDUCTANCE DIRECTION	(A_E) ELLIPSE AREA	(A_Z) ZONE AREA	AVERAGE ZONE EFFICIENCY η_2
(1)					
(2)					
(3)					
(4)	– – – –	– – – –	TOTAL SHIELD AREA		

4.0 Test Results

Twelve sample honeycomb shields were tested to verify the mathematical model which was developed in the February 1975 report. The physical parameters of these samples are listed in Table I. Samples 1 thru 6 are of Hexcel Corporation Kraft paper*, while samples 7 thru 12 are of American Cyanamid 6061 aluminum. Samples having a surface emissivity of 0.86 were painted with 3-M Corporation Nextel 101-C10 black paint (see Figure 26 for spectral data). Samples 9 and 12 were bare aluminum (i.e., as received) while samples 5 and 6 were coated at GSFC with an aluminum pigmented coating.

Tests were performed in vacuum at a pressure of less than 5×10^{-5} in a configuration as noted in Figure 17.

The honeycomb test sample, hot plate, and cold plate formed a sandwich assembly which was insulated from the surroundings with an aluminized mylar thermal blanket. The hot and cold plates were instrumented with up to four thermocouples each, and each honeycomb sample was instrumented with six thermocouples. Two of the six thermocouples on the honeycomb shield were fixed to the centermost cell, one on the hot side and one on the cold side. The remaining four were positioned on the hot side, two on a high conductance cell row, and two on a low conductance cell row.

Both the hot and cold sinks were coated with 3M 101-C10 black paint. The hot plate was heated with Minco Corporation strip heaters, and the cold sink, a flat-faced stainless steel tank, was filled with liquid nitrogen.

*Hexcel Corporation Part Nos. KP-1/4-80(11)E and KP-3/8-80(11)E.

The honeycomb samples were bonded into square aluminum frames having an aperture area of 68 square inches. The frames were fabricated of modified angle stock of 0.125 inch thickness welded in all four corners. The honeycomb cells were bonded to the frame with a fillet of Wakefield Deltabond 154-Q/B4 thermally conductive epoxy at each* frame/honeycomb interface. For tests in the conductively coupled configuration, Minco Corporation strip heaters were fixed to the perimeter of the honeycomb frame.

4.1 Conductively Isolated Shield Tests

Tests were performed on twelve samples as noted in Table II. Only eight of these could be compared with the mathematical model, though, since the model requires a diffuse surface. Samples 9 and 12 without question do not have diffuse surfaces, and the results for samples 5 and 6 would imply a significant specular component (note: the mathematical model predicts a higher efficiency for reduced emissivity).

The difference between predicted and measured values for hot plate power for those samples painted with 3-M 101-C are listed in Table II. The differences are all less than 5% except for sample 11 (6.7%). The table also notes the predicted and measured rate of cell temperature for both the hot and cold end. It is apparent that both the predicted temperatures and predicted power dissipation compare favorably with the measured values. The obvious conclusion is that the model** provides an accurate representation of the power transfer through the shield.

*It was not possible to bond each cell to the frame for samples 8 and 10 because of the small cell size.

**The parameters which were input to the computer model were the actual test parameters.

The results for the samples painted with GSFC aluminum paint (5 and 6) were surprising in that the power dissipation was expected to be equal to or slightly lower than that for the equivalent sample painted with 3-M black. Since the measured power dissipation is 20 to 30% higher than expected, a strong specular component is suspected to exist for the aluminum paint.

The general performance of the samples having an "as received" aluminum coating (9 and 12) was as expected. A specular, low emissivity honeycomb surface will allow almost all radiated energy to pass through it, and without question, aluminum in this form is highly specular and has a low emissivity.

4.2 Conductively Coupled Shield Results

Six samples were tested in the conductively coupled mode, of which four were directly comparable to the model/algorithm. The results for samples 9 and 12 are presented for academic interest only.

The results for samples 7, 8, and 10 compared favorably with the model/algorithm without any modifications. The results noted in Table III for samples 8 and 10 include a contact resistance (value noted in the table) between the honeycomb frame and the honeycomb shield, but this resistance is not absolutely required to make a reasonable estimate of shielding efficiency. The magnitude of the difference is presented in Figures 20 and 22. These figures clearly illustrate, though, that good coupling between the frame and honeycomb is highly desirable.

The variance between measured and predicted power for sample 11 could not be resolved by adding contact resistance. In fact, just

the opposite was true. The predicted temperatures and power dissipation would agree with the measured values only if the coupling between the frame and honeycomb were increased rather than decreased. Figure 24 notes the difference in performance between the baseline model and that modified with the negative contact resistance.

The model/algorithm appears to be more than adequate for evaluating the approximate performance of a honecomb shield in the conductivity coupled configuration. Where it is important to know the thermal transfer characteristics to better than 15% (using $\sigma A_1 T_1^4$ as the base), a test program is recommended.

HONEYCOMB TEST SAMPLE PHYSICAL PARAMETERS

TABLE I

SAMPLE NO.	PHYSICAL PARAMETERS							
	W (in.)	H (in.)	k (btu/hr ft.°F)	t (in.)	L	N_c	Total Hemisperical Emissivity ϵ	Surface Description
1	.250	.375	0.16	0.008	2.60	2.43	.86	3-M 101-C10
2	0.250	1.00	0.16	0.008	6.93	17.3	.86	3-M 101-C10
3	0.375	0.375	0.16	0.008	1.73	2.42	.86	3-M 101-C10
4	0.375	1.00	0.16	0.008	4.62	17.3	.86	3-M 101-C10
5	0.250	1.00	0.16	0.008	6.93	17.3	.86	3-M 101-C10
6	0.375	1.00	0.16	0.008	4.62	17.3	—	GSFC Aluminum Paint
7	0.375	0.625	80.0	0.005	2.89	0.02	—	GSFC Aluminum Paint
8	0.125	1.00	80.0	0.001	13.9	0.24	.86	3-M 101-C10
9	0.375	0.625	80.0	0.005	2.89	0.02	—	Aluminum as received
10	0.093	0.750	80.0	0.00094	14.0	0.165	.86	3-M 101-C10
11	0.750	0.500	80.0	0.002	1.15	0.04	.86	3-M 101-C10
12	0.750	0.500	80.0	0.002	1.15	0.04	—	Aluminum as received
ALTERNATES								
1A	.250	.250	.16	.008	1.73	1.08		
2A	.250	.687	80.0	0.0025	4.76	0.05		
3A	0.187	0.625	80.0	0.0025	5.77	0.04		
5A	0.250	0.625	80.0	0.00135	4.33	0.08		

INSULATED FRAME TEST RESULTS
TABLE II

Sample	Hot Plate Temp. °C	Cold Plate Temp. °C	Q_1 Predicted watts	Q_1 Measured watts	Power Difference %	Cell Temperatures °C			
						Hot End		Cold End	
						Predicted	Measured	Predicted	Measured
1	25.4	-167.4	10.02	9.95	-.71	-14.1	-12.7	-28.6	-23.5
2	24.7	-174.4	7.21	7.28	+0.97	- 4.2	- 3.9	-43.9	-40.9
3	26.6	-158.8	11.20	11.23	+0.24	-13.0	-10.9	-27.0	-23.8
4	25.7	-172.3	7.75	7.87	+1.53	- 2.3	0.2	-44.2	-43.6
5(2)	26.1	-188.6	--	8.77	--	--	- 7.2	--	-31.1
6(4)	25.3	-184.8	--	10.02	--	--	-14.5	--	-28.5
7	25.2	-162.0	10.31	10.66	+3.44	-21.0	-16.7	-21.1	-20.8
8	25.1	-157.1	9.49	9.82	+3.51	-20.6	-17.9	-21.3	-21.0
9(7)	26.5	-137.3	--	16.00	--	--	-11.0	--	-11.4
10	25.1	-156.5	9.51	9.65	+1.47	-20.6	-19.6	-21.1	-21.8
11	27.1	-183.7	13.02	12.14	-6.74	-20.1	-19.7	-20.4	-20.9
12(11)	25.8	-171.5	--	16.78	--	--	-19.0	--	-19.6

HEATED FRAME TEST RESULTS
TABLE III

Sample No.	Frame Temp.	Hot Plate Temp.	Cold Plate Temp.	Power (Watts) Predicted Q_1	Predicted Q_2	Predicted Q_{sink}*	Measured Q_1	Measured Q_2*	Measured Qsink	Differences Q_1	Differences Q_2	Differences Qsink	Contact Resistance to Frame (°C/watts)
7	25.6	25.7	-129.5	4.15	16.03	11.88	5.2	16.5	11.3	-1.0	-0.5	+0.6	zero
8	24.7	27.8	-139.8	3.30	15.73	12.43	4.0	16.1	12.1	-0.7	-0.4	+0.3	4.71×10^{3}
9	27.7	25.3	-138.6	--	--	--	13.7	17.5	3.8	--	--	--	--
10	26.0	27.0	-137.1	2.54	15.60	11.4	4.2	15.6	11.4	-1.7	+0.9	+2.6	6.31×10^{3}
11	26.6	28.3	-174.4	10.12	16.12	6.00	8.9	16.13	7.4	+1.2	-0.2	-1.4	-1.2×10^{3}
12	28.7	26.1	-168.1	--	--	--	15.4	18.4	3.0	--	--	--	--

Note: The predicted parameter Q_{sink} and the measured parameter Q_2 are inferred:

$$Q_{sink} = Q_2 - Q_1$$

$$Q_2 = Q_{sink} + Q_1$$

5.0 Sample Analysis

The following paragraphs will illustrate the use of the design graphs by examining a potential application for the honeycomb thermal shield. The information for this analysis was derived from a brief proposal titled "Experiment Description for Large Area Modular Array (LAMAR) for SPACE SHUTTLE", by Paul Gorenstein, dated 25 November 1974. The schematic picture of Figure 22 illustrates the general arrangement of the instrument and notes the location of twenty-one square "mechanical collimators", each 18 inches on a side and 6 inches deep. The apparent function of the collimators is thermal shielding. Other information presented in the description which is required for the honeycomb shield design is:

1) Instrument temperature: -25° to +30°C not observing narrower TBD when observing.
2) Field of View: 1.6° FWHM
3) Total Power Consumption: 150 to 200 watts
4) Energy Range: 0.1 to 4 kev

The first step is to determine if a high efficiency thermal shield such as aluminized mylar can be used in place of the honeycomb shield. Generally this is a decision for the Principal Investigator, but from the stated energy range, it can be assumed that the honeycomb shield is required.

The second step is to select a reasonable cell configuration if possible. The specification calls for a 1.6° Full Width Half Maximum field-of-view. This does not necessarily mean that the honeycomb shield has a view of 1.6° FWHM. Typically the honeycomb shield must be much more transparent so as not to decrease the detector solid angle significantly. For example, the OSO-8 Wisconsin Soft X-Ray Instrument employed a honeycomb shield of 31 degrees FWHM with a detector of 2 degrees FWHM. Using this as a basis for

specifying the LAMAR shield, the honeycomb shield FOV must be 25 degrees, minimum:

$$\frac{(W)}{(H)} = \tan 25° = 0.466$$

and for H = 6.0 inches, W = 2.8 inches

Since the cell width noted above is unusually large compared to sizes which are commercially available, the heat loss will be first estimated for a more practical size:

W = 0.75 inch $T_1 = 25°C$

H - 1.75 inch $T_2 = -273°C$

k = 80 BTU/hr ft.°F $\varepsilon = 1.0$

t = 0.008 inch

From the above, the dimensionless parameters can be determined:

L = 4.04

$N_c = 0.106$

Field of View = 23° FWHM

5.1 Conductively Isolated Shield

In the following analysis it is assumed that the driving system requirement is that the instrument heat loss must be at or below the level of its electrical power dissipation.

The efficiency value required to determine the total heat loss can be found in Figure 6. For the stated values of L and N_c, the efficiency is 0.5. Using the relationship of Paragraph 3.3:

$$QRAD(1) = (1-\eta)(\sigma A_1)(T_1^4-T_2^4)$$

$$QRAD(1) = (1-0.5)(5.67\text{x}10^{-12})(2090\ cm^2)(298^4)$$

$$QRAD(1) = 46.8 \text{ watts}$$

For 21 modules, the total power requirement is 983 watts which is far in excess of the proposed maximum electrical power dissipation of 200 watts. Even with T_1 reduced to the low limit of -25°C, the same shield would require 472 watts for 21 modules.

If the external heat loss from the module must be balanced by its internal power dissipation, then T_1 must be reduced to -25°C and N_c must be increased by fabricating a multi-layer shield which has several layers which are conductively decoupled. Also, L must be increased such that η is 0.80 for large values of N_c.

It is possible to calculate the value of L required to yield an efficiency of 0.8 by using the method presented in the February 1975 report. The method estimates the value of η resulting from stacking two low conductance shields one on top the other:

$$\eta_{a+b} = 1 - \frac{1}{\frac{\eta_a}{1-\eta_a} + \frac{\eta_b}{1-\eta_b} + 1}$$

From Figure 6 $\eta = 0.71$ for $L = 8.0$.

Substituting $\eta_a = \eta_b = 0.71$ into the above equation yields

$\eta_{a+b} = 0.83$. Therefore it can be inferred that $\eta = 0.83$ for a low conductance shield of $L = 16.0$.

From the definition of L, W may be determined:

$$W = H(2 \sin 60)/L = 0.65 \text{ inch}$$

As a practual matter, the shield may be assembled of six layers, each one inch thick. The field of view of this assembly is now 6.2° FWHM rather than the goal of 25°.

Recalculating the heat loss per module for $\eta = 0.83$, and $T_1 = -25°C$:

QRAD(1) = 7.6 watts

or 160.4 watts for 21 modules.

5.2 Conductively Coupled Shield

Given the example of Paragraph 5.1, it is difficult to imagine an application for the instrument using the conductively coupled configuration which yields a reasonable power dissipation. But, for the sake of illustration, assume <u>one</u> module is shielded in this fashion. Using the algorithm presented in Paragraph 3.4 and the shield parameters specified in Paragraph 5.0:

<u>STEP 1</u> W = 0.75 inch $T_o = 25°C$

H = 1.75 inch $T_1 = 25°C$

k = 80. BTU/hr Ft°F $T_2 = =273°C$

t = 0.008 inch $\varepsilon = 1.0$

Shield Dimensions = 18 x 18 inches

<u>STEP 2</u> L = 4.04

$N_c = 0.106$

$T_o/T_1 = 1.0$

<u>STEP 3</u> N = 12 for high conductance direction

N = 7 for low conductance direction

<u>STEP 4</u> Refer to the graphs for L = 4 in Figures 12 and 13.

<u>STEP 5</u> 0.52

<u>STEP 6</u> See Tables WS-1 thru WS-4. <u>Note:</u> The cell numbers and dimensions in Table WS-2 are not always equal to those of Table WS-1.

STEP 7 $\eta_1)_{ave} = 0.68$

$\eta_2)_{ave} = 0.29$

STEP 8 $QRAD(1) = (1-0.68)(\sigma)(2090\ cm^2)(298)^4 = 29.9$ watts

$QRAD(2) = (1-0.29)(\sigma)(2090 cm^2)(298)^4 = 66.4$ watts

$Q_{sink} = QRAD(2) - QRAD(1) = 36.5$ watts

TABLE WS – 1 (Sample Problem)

LINE NO.	η_1	LOW CONDUCTANCE CELL NO.	LOW CONDUCTANCE DIM. (R)	HIGH CONDUCTANCE CELL NO.	HIGH CONDUCTANCE DIM. (S)
1	0.74	1	1.3 inch	1.6	1.2
2	0.58	4	5.2 inch	5.9	4.4
3	0.54	6	7.8 inch	8.4	6.3
4	--	---	---	---	---

TABLE WS – 2 (Sample Problem)

LINE NO.	η_2	LOW CONDUCTANCE CELL NO.	LOW CONDUCTANCE DIM. (R)	HIGH CONDUCTANCE CELL NO.	HIGH CONDUCTANCE DIM. (S)
1	0.22	1	1.3 inch	1.6	1.2
2	0.38	4	5.2 inch	5.9	4.4
3	0.44	6	7.8 inch	8.4	6.3
4	---	---	---	---	---

(Sample Problem)

TABLE WS – 3 (Based on values in TABLE WS – 1)

AREA ID.	(D_L) ELLIPSE DIA. IN LOW CONDUCTANCE DIRECTION	(D_H) ELLIPSE DIA. IN HIGH CONDUCTANCE DIRECTION	(A_E) ELLIPSE AREA	(A_Z) ZONE AREA	AVERAGE ZONE EFFICIENCY η_1
(1)	2.4	5.4	10.2 in^2	10.2 in^2	0.54
(2)	7.6	9.2	54.9	44.7	0.56
(3)	5.4	15.6	188.7	133.8	0.66
(4)	— — — —	— — — —	TOTAL SHIELD AREA 324.0	135.3	0.74

(Sample Problem)

TABLE WS – 4 (Based on values in TABLE WS – 2)

AREA ID.	(D_L) ELLIPSE DIA. IN LOW CONDUCTANCE DIRECTION	(D_H) ELLIPSE DIA. IN HIGH CONDUCTANCE DIRECTION	(A_E) ELLIPSE AREA	(A_Z) ZONE AREA	AVERAGE ZONE EFFICIENCY η_2
(1)	2.4	5.4	10.2	10.2	0.44
(2)	7.6	9.2	54.9	44.7	0.41
(3)	15.4	15.6	188.7	133.8	0.30
(4)	— — — —	— — — —	TOTAL SHIELD AREA 324.0	135.3	0.22

APPENDICIES

APPENDIX A

NOMENCLATURE

A_1	area of honeycomb
H	honeycomb cell height; also cylinder height
k	thermal conductivity of honeycomb wall
L	ratio of 1.73 H/W
N	number of cells in an isolated row
N_c	thermal coupling parameter $\left[\frac{H^2 \sigma T_1^3}{kt}\right]$
QRAD(1)	net heat transfer from A_1
QRAD(2)	net heat transfer from A_2
Q_{sink}	net heat transfer from sink at T_o
t	honeycomb cell wall thickness
T_o	temperature of conductive sink
T_1	temperature of radiative source
T_2	temperature of radiative sink
W	honeycomb width across flats
ε	surface emissivity
σ	Stefan-Boltzman constant
η	shielding efficiency

APPENDIX B

Figures

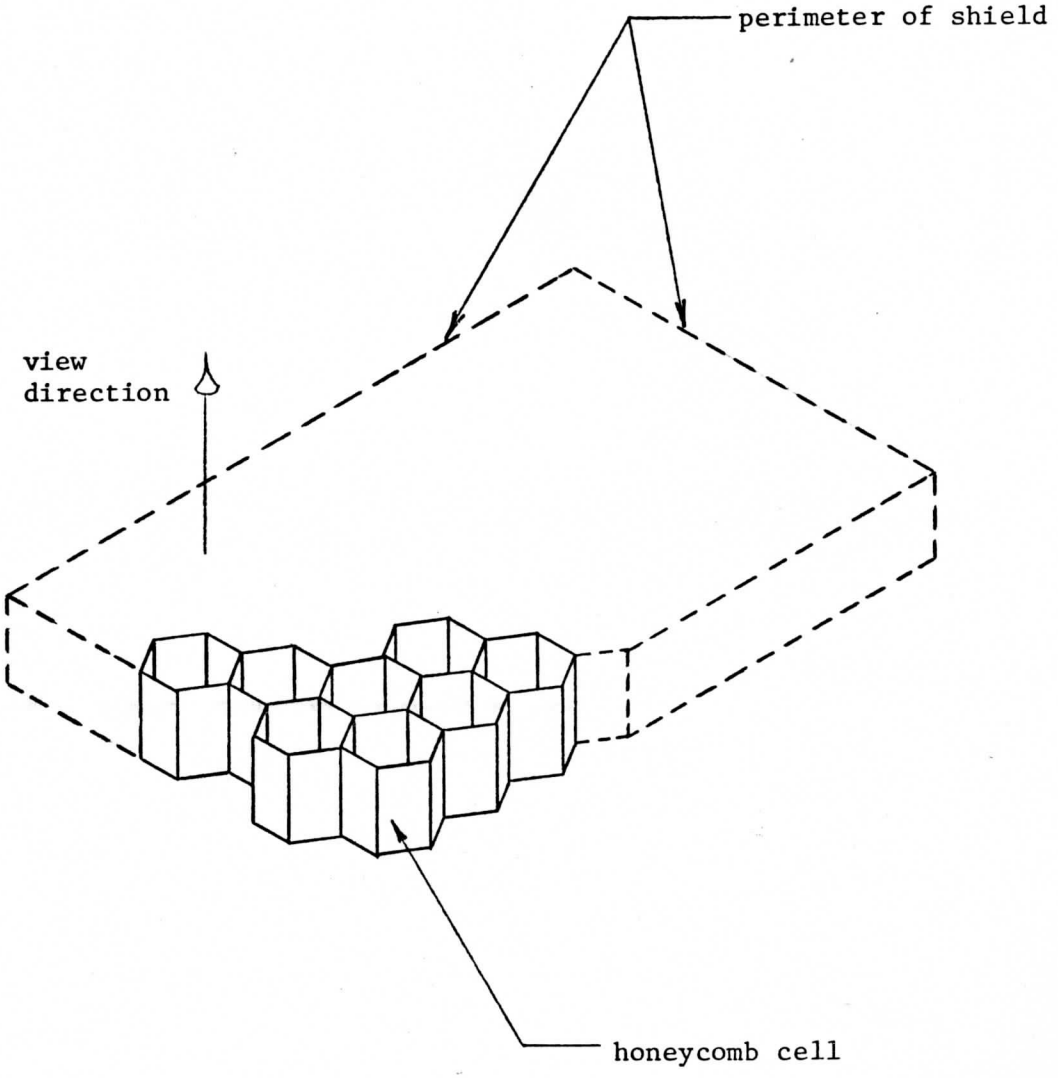

Figure 1. Honeycomb Thermal Shield Schematic

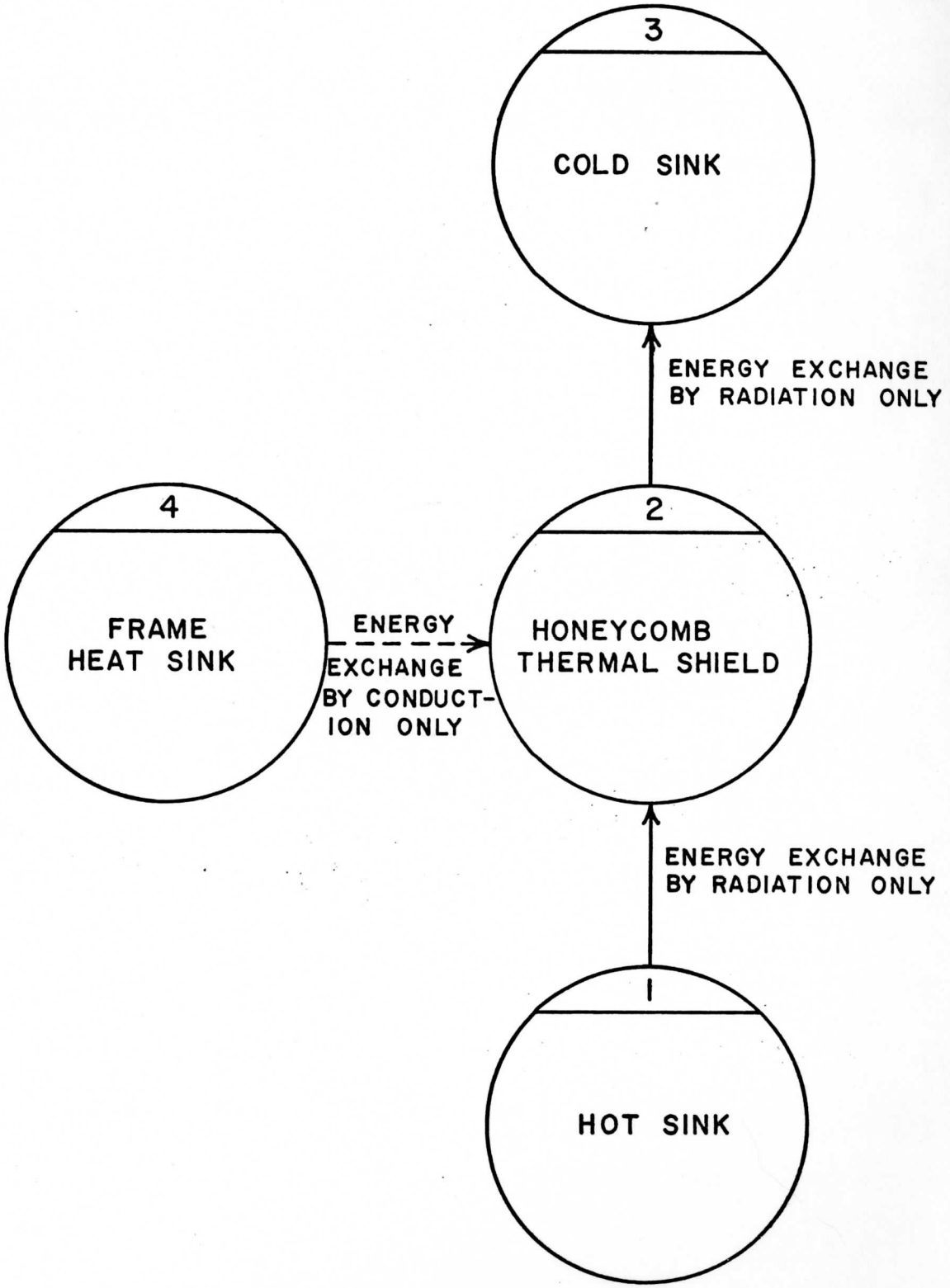

HEAT FLOW PATH

Figure 2

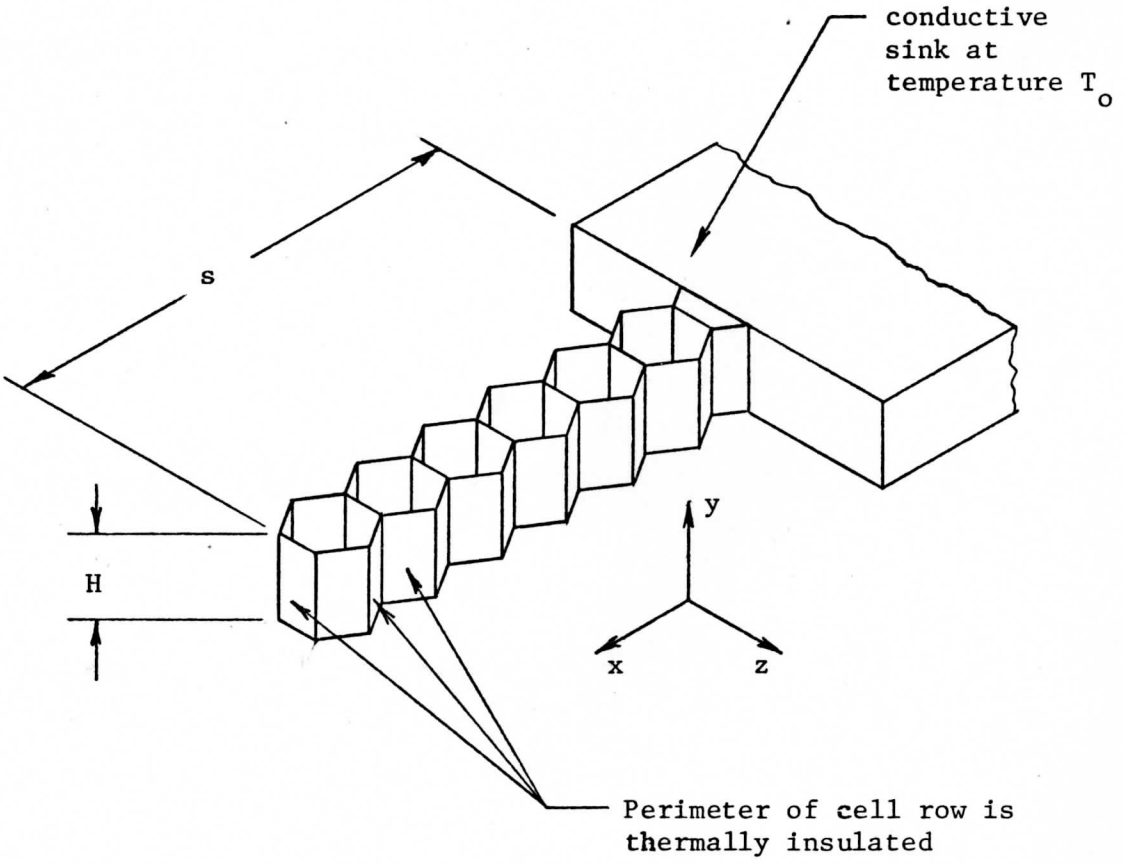

Figure 3. Isolated Cell Row, High Conductance Direction

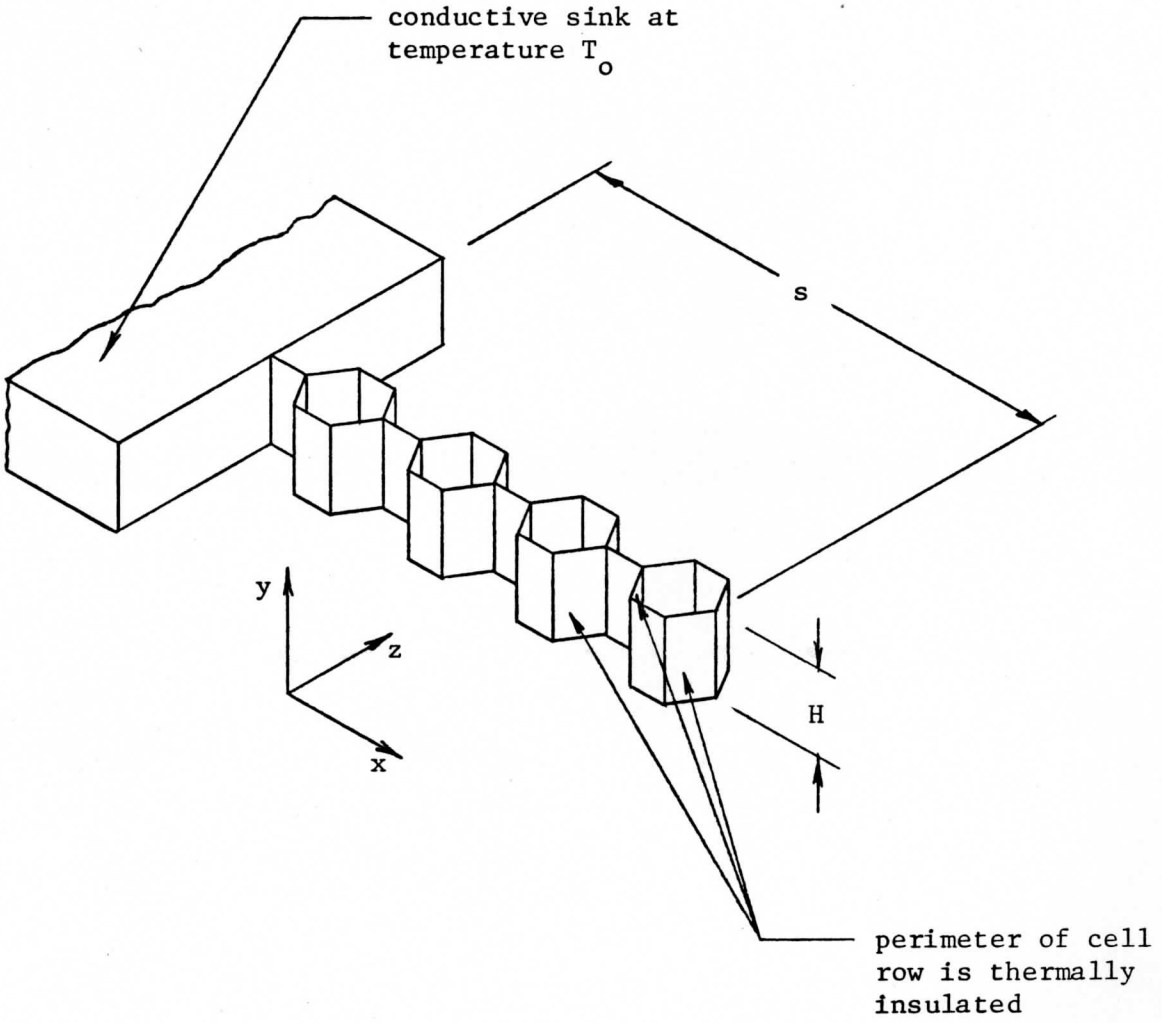

Figure 4. Isolated Cell Row, Low Conductance Direction

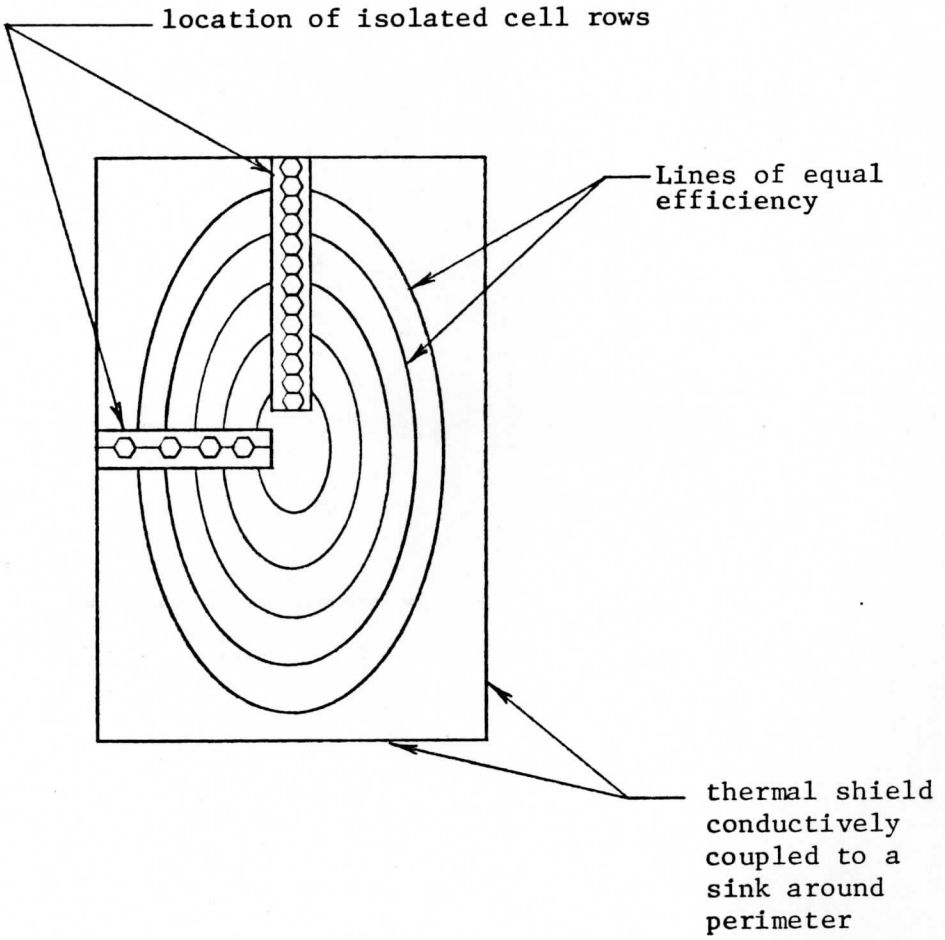

Figure 5. Location of Isolated Cell Rows in a Typical Honeycomb Thermal Shield

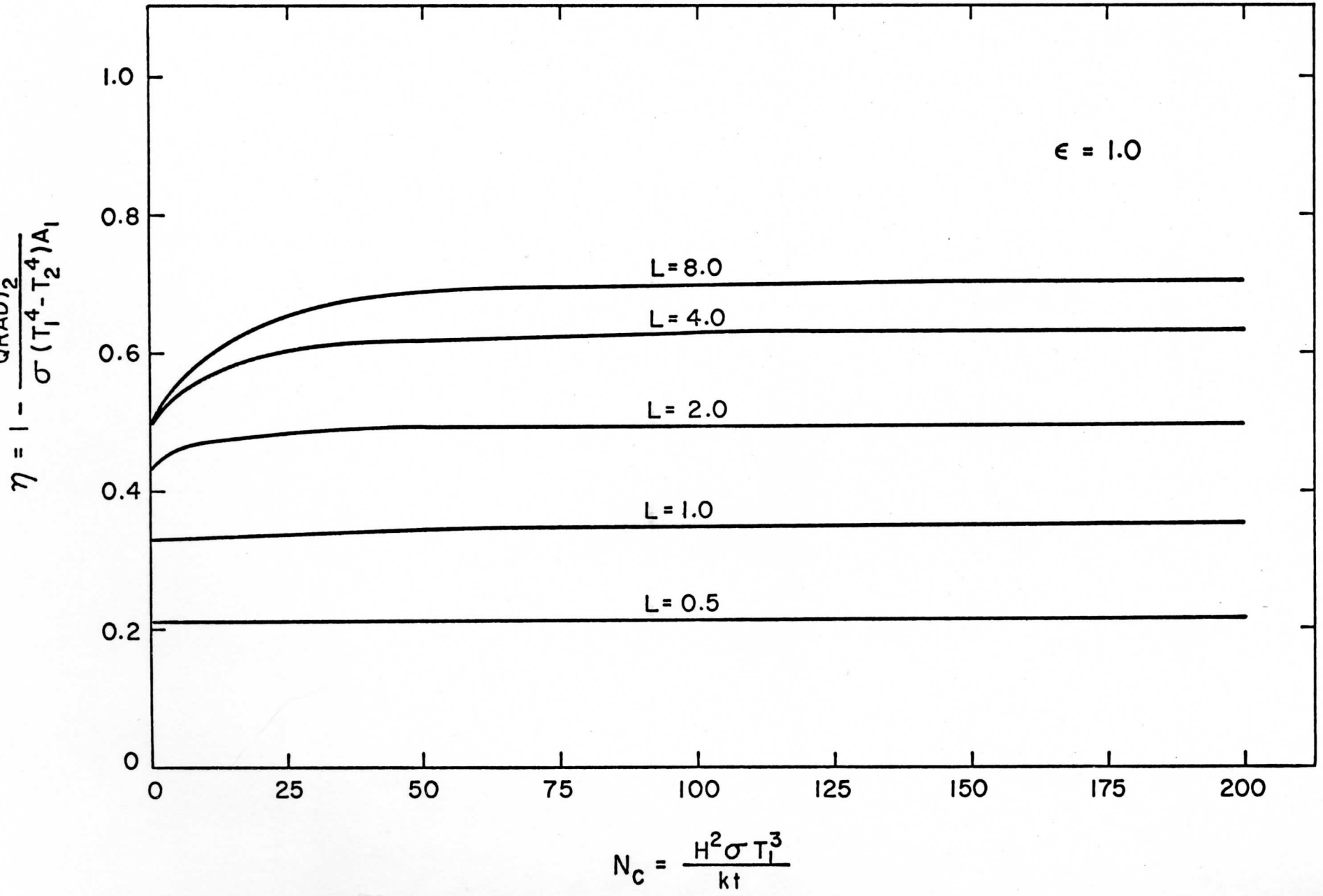

Figure 6. Efficiency vs N_c for Isolated Cells with $\epsilon = 1.0$

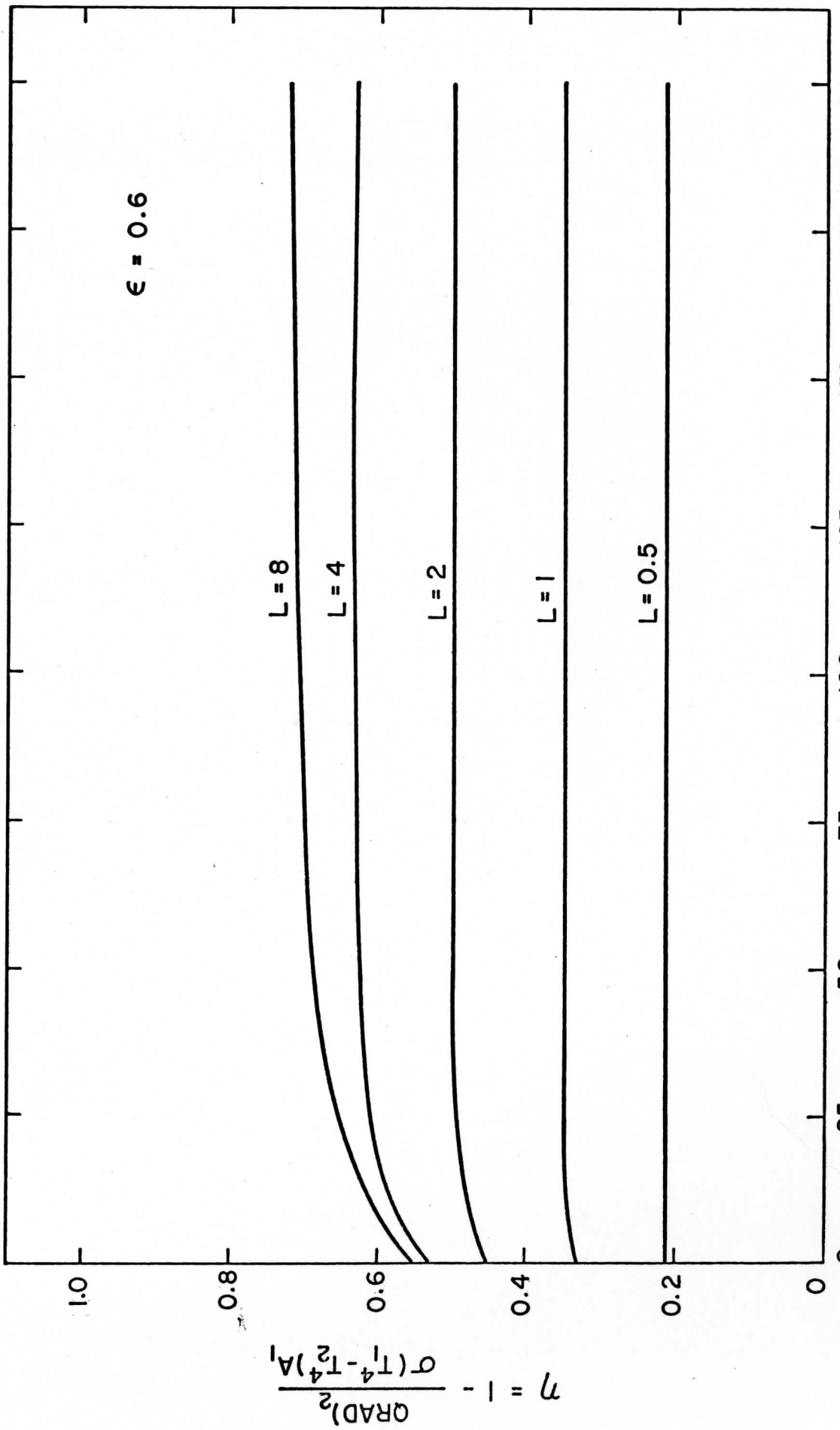

Figure 7. Efficiency vs N_c for Isolated Cells with $\epsilon = 0.6$

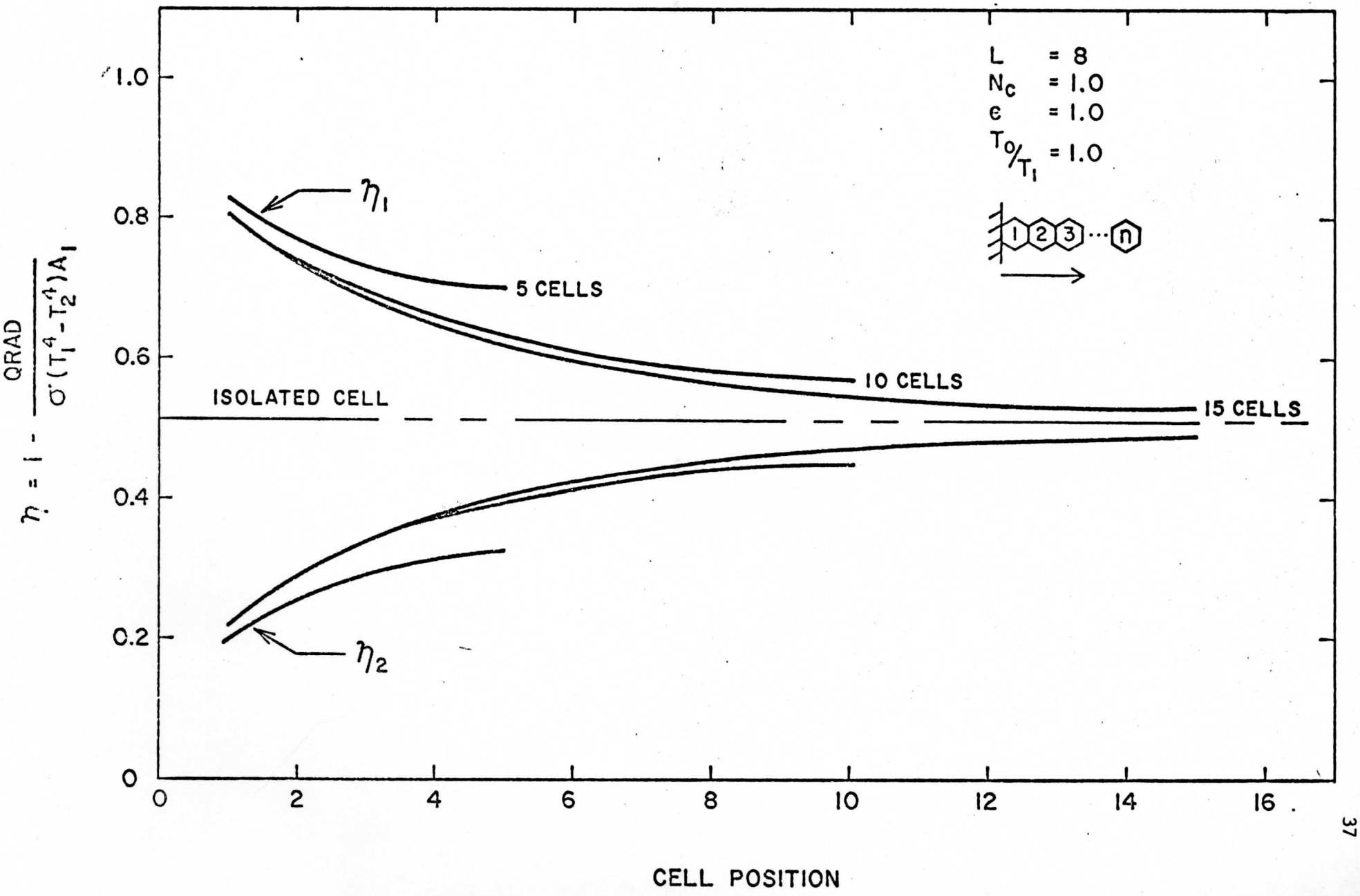

Figure 8. Efficiency vs Cell Position and Number of Cells per Row for L = 8.

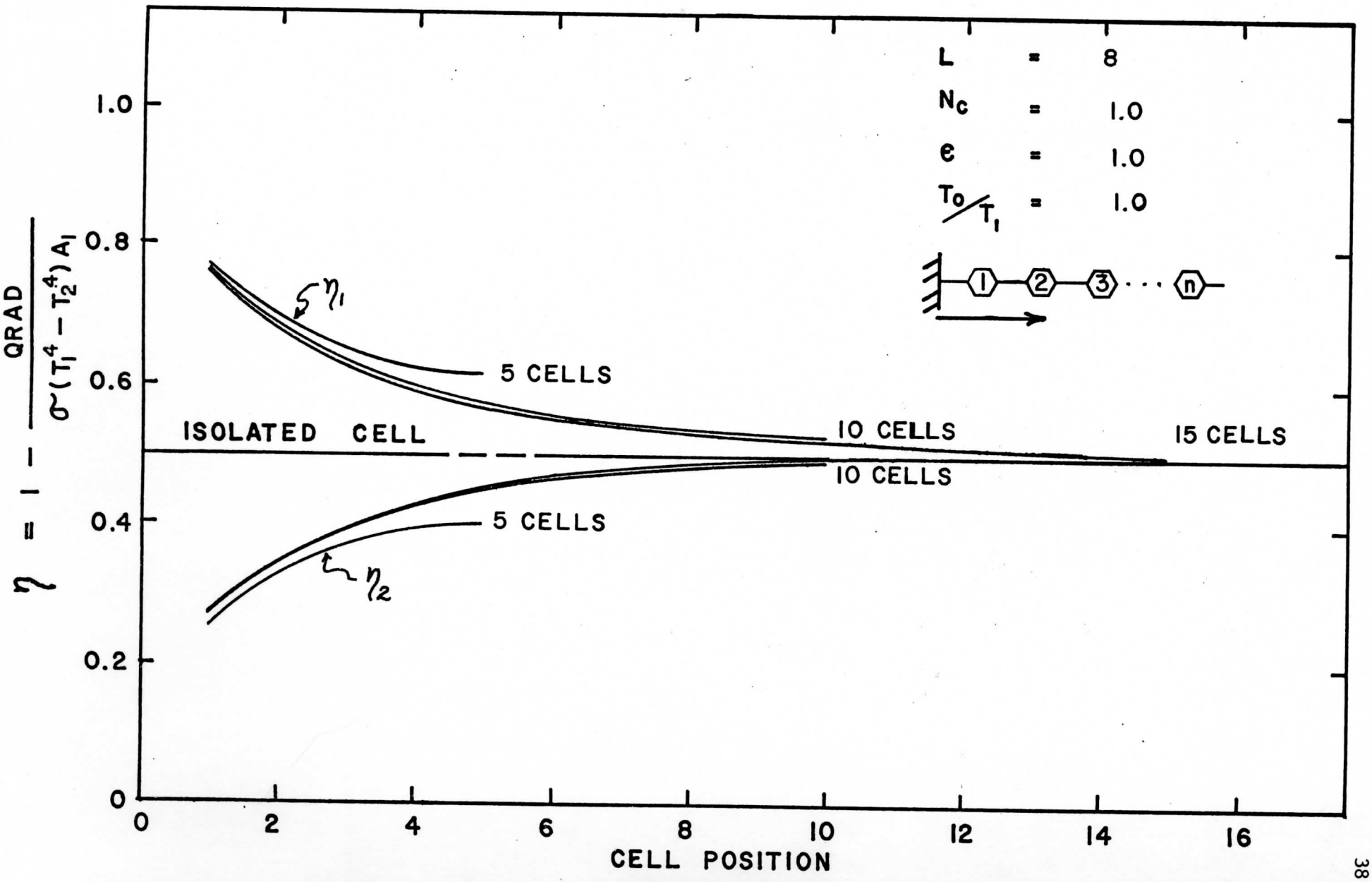
L = 8
N_c = 1.0
e = 1.0
T_o/T_1 = 1.0
1
2
3
n
$\eta = 1 - \frac{QRAD}{\sigma(T_1^4 - T_2^4)A_1}$
η_1
η_2
5 CELLS
10 CELLS
15 CELLS
ISOLATED CELL
5 CELLS
10 CELLS
0
0.2
0.4
0.6
0.8
1.0
0
2
4
6
8
10
12
14
16
CELL POSITION

Figure 9

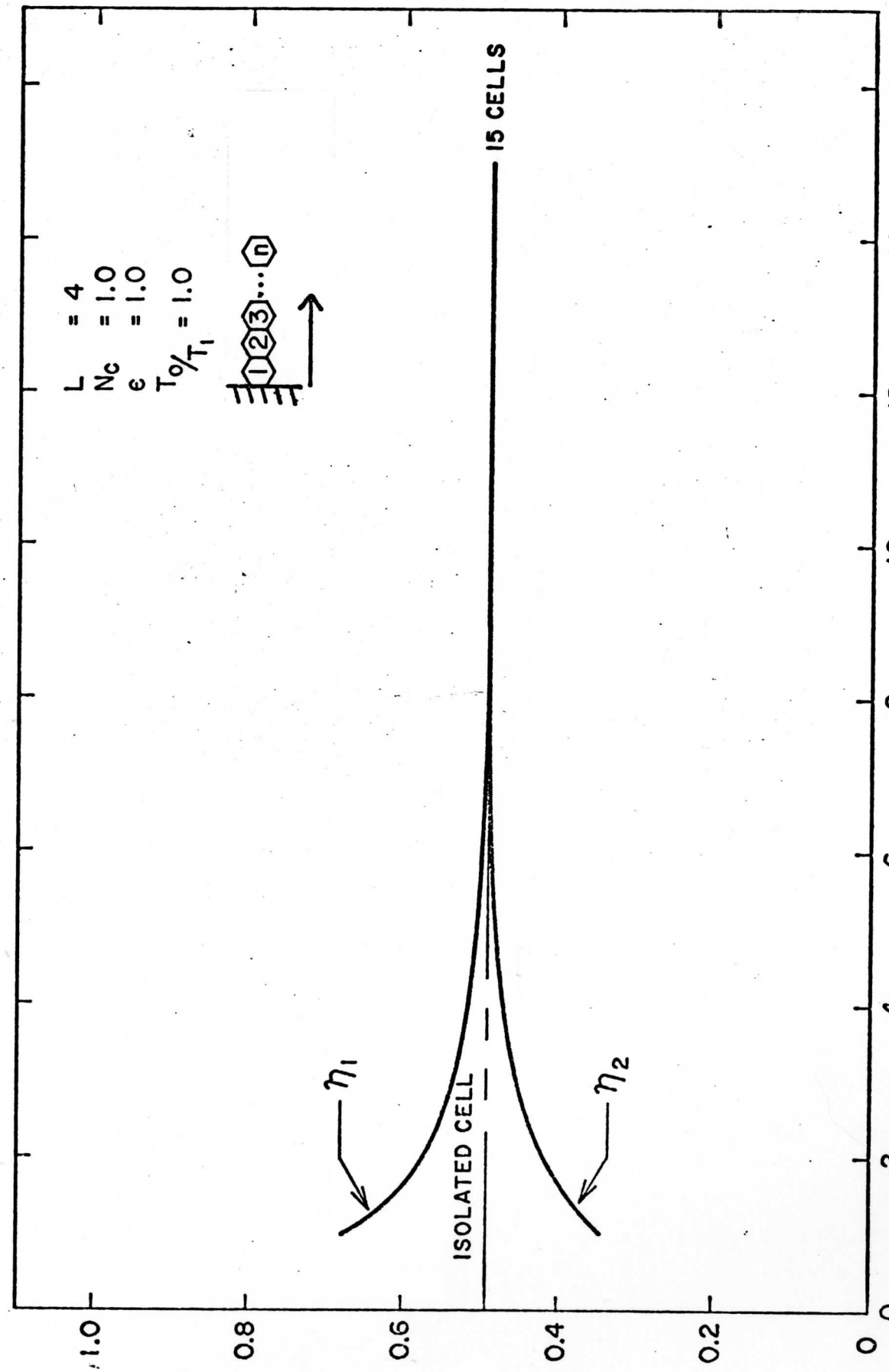

Figure 10. Efficiency vs Cell Position and Number of Cells per Row for L = 4.

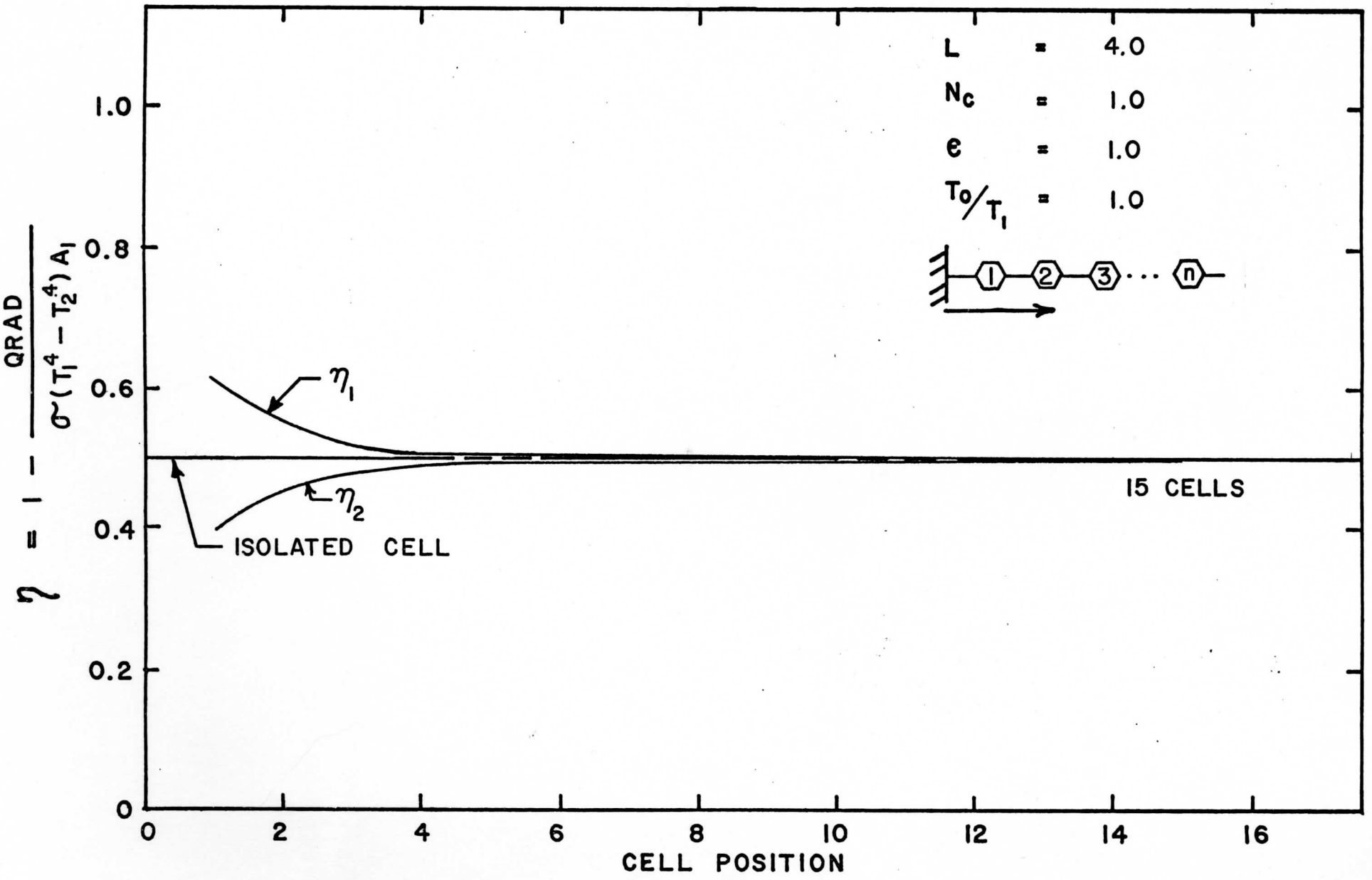

Figure 11. Efficiencey vs. Cell Position

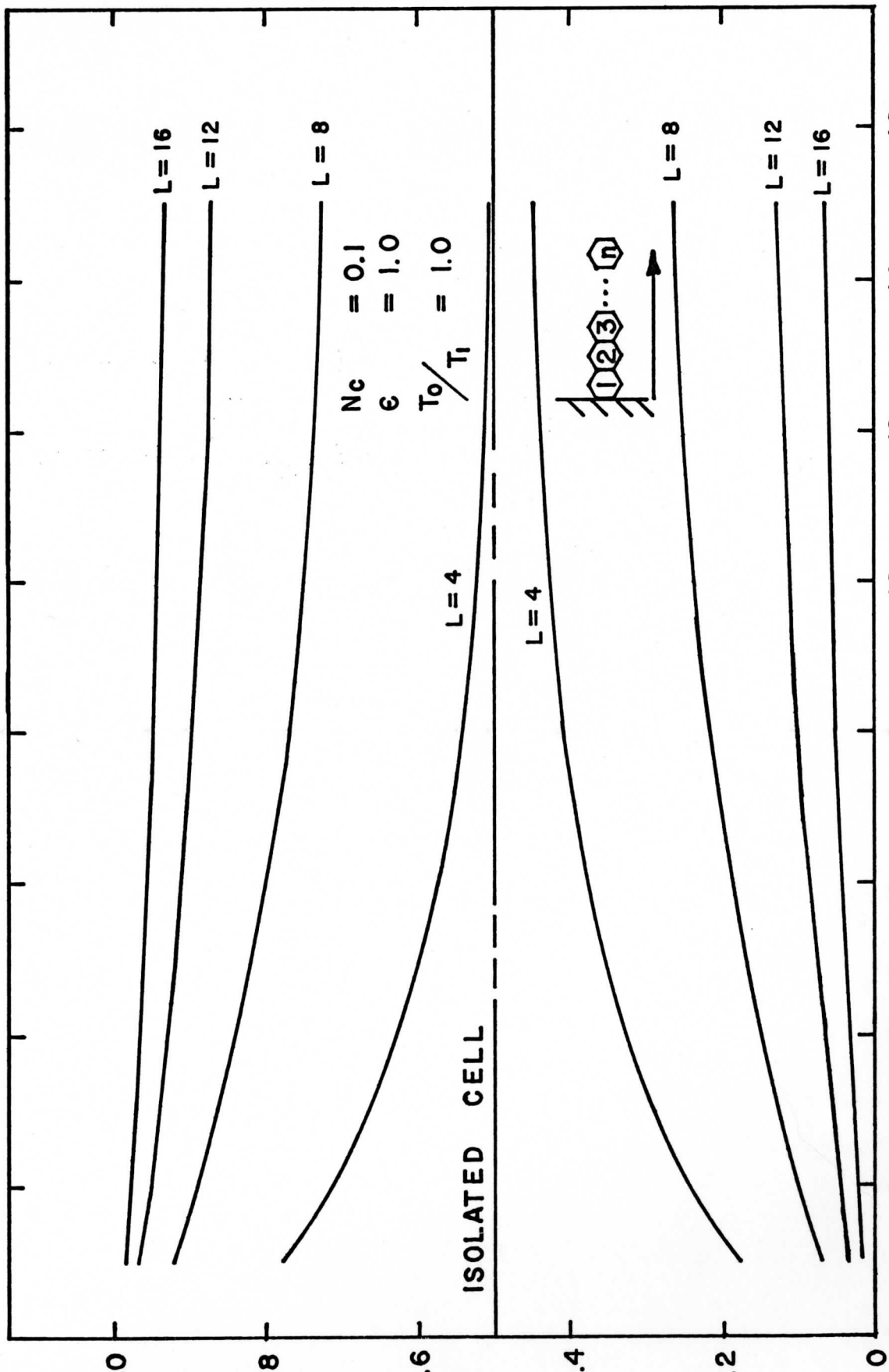

Figure 12. Efficiency vs. Cell Position for N_c = 0.1

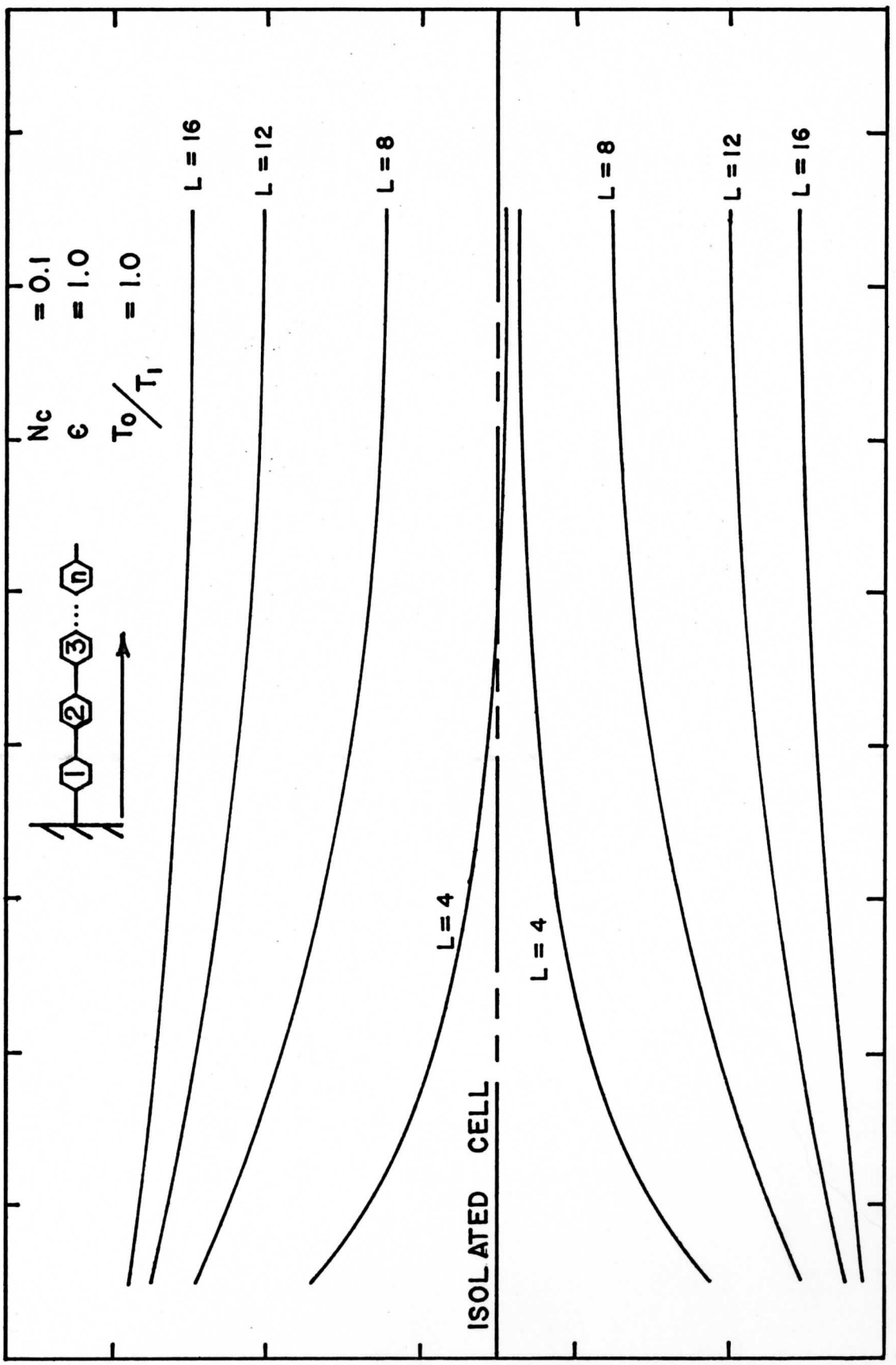

Figure 13. Efficiency vs. Cell Position for N_c = 0.1

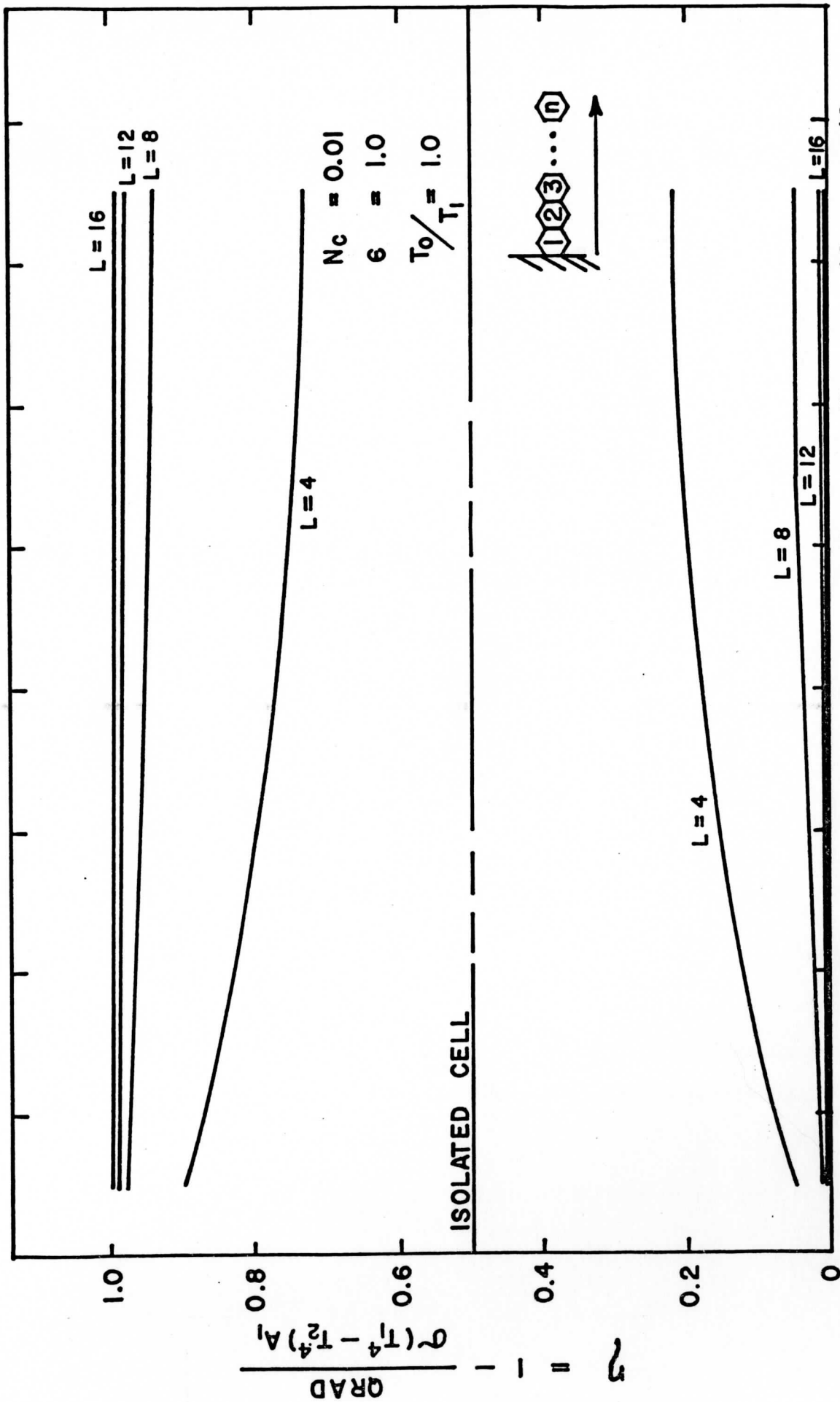

Figure 14. Efficiency vs. Cell Position for $N_c = 0.01$

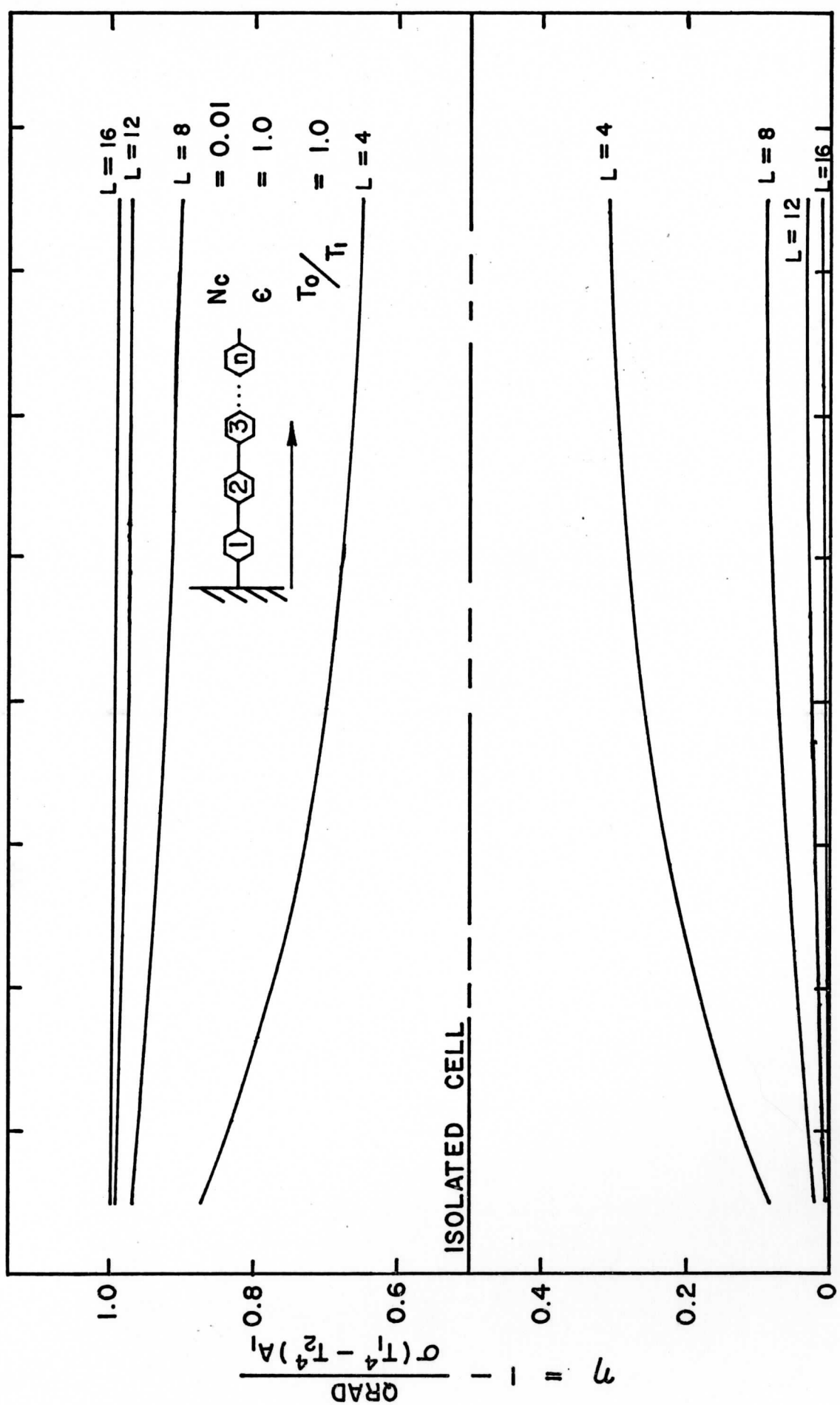

Figure 15. Efficiency vs. Cell Position for N_c = 0.01

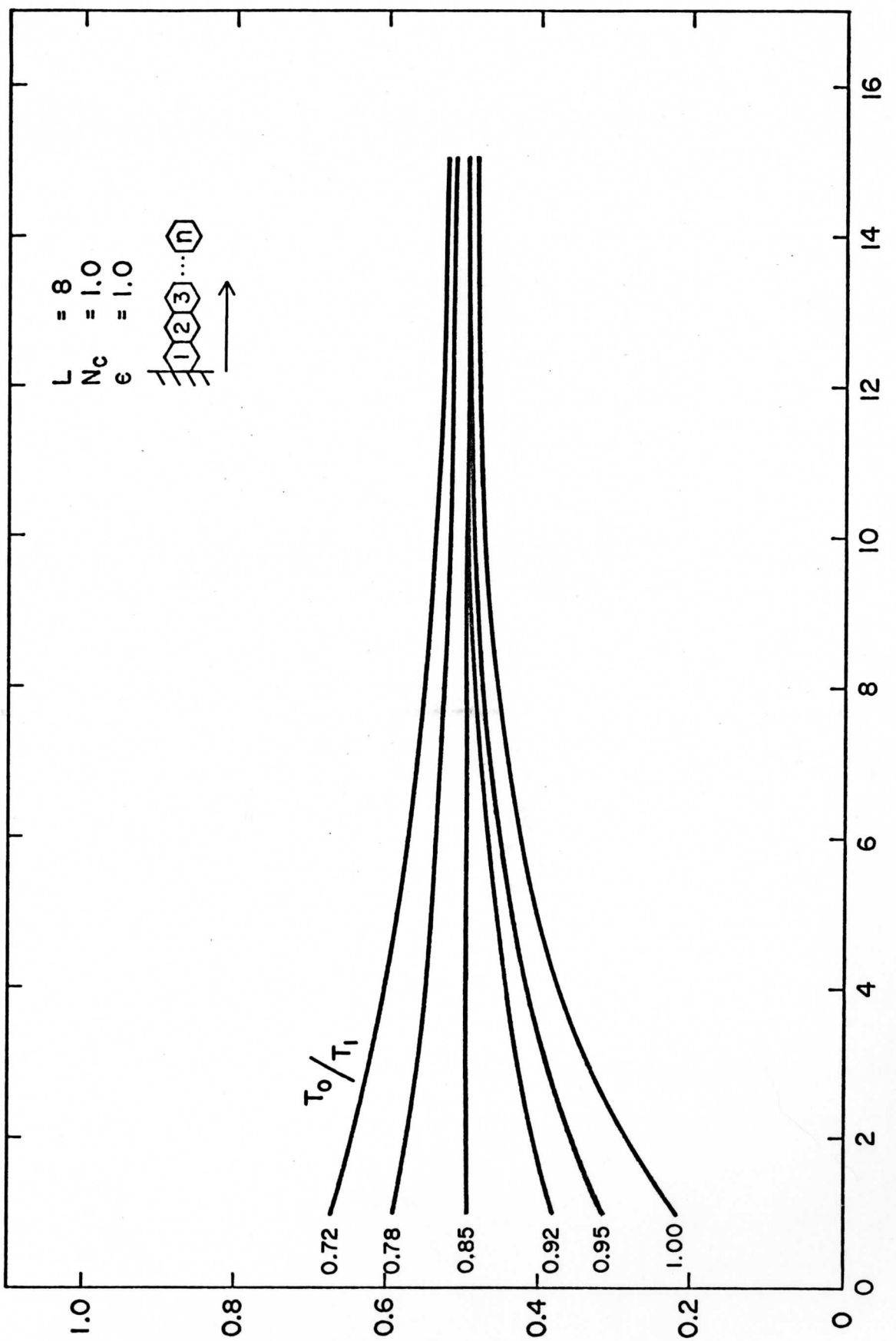

Figure 16. Efficiency vs cell position and (T_o/T_1) for L = 8.

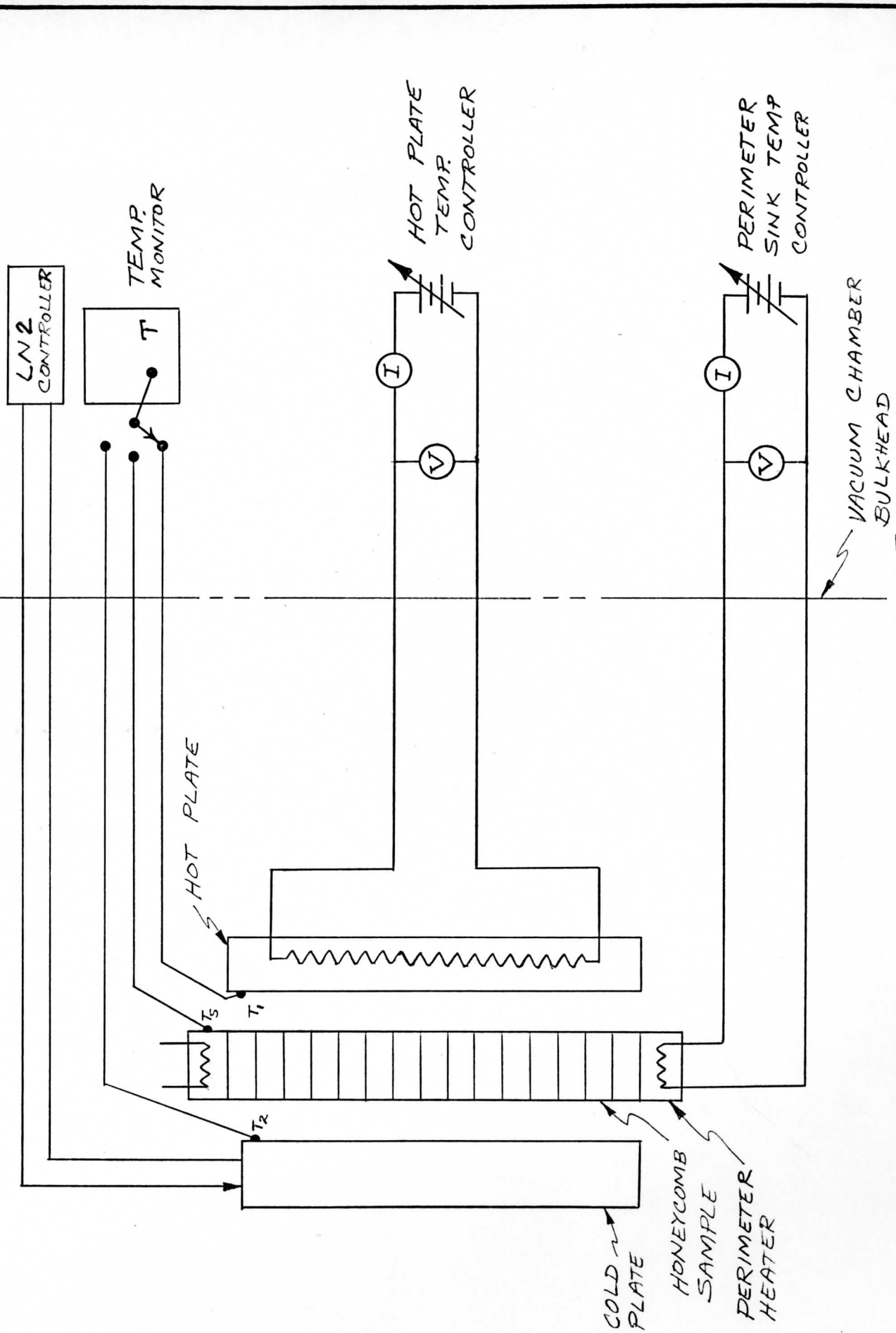

TEST FIXTURE
FIGURE 17

	REVISION	DRAWING NO.	SHEET 7

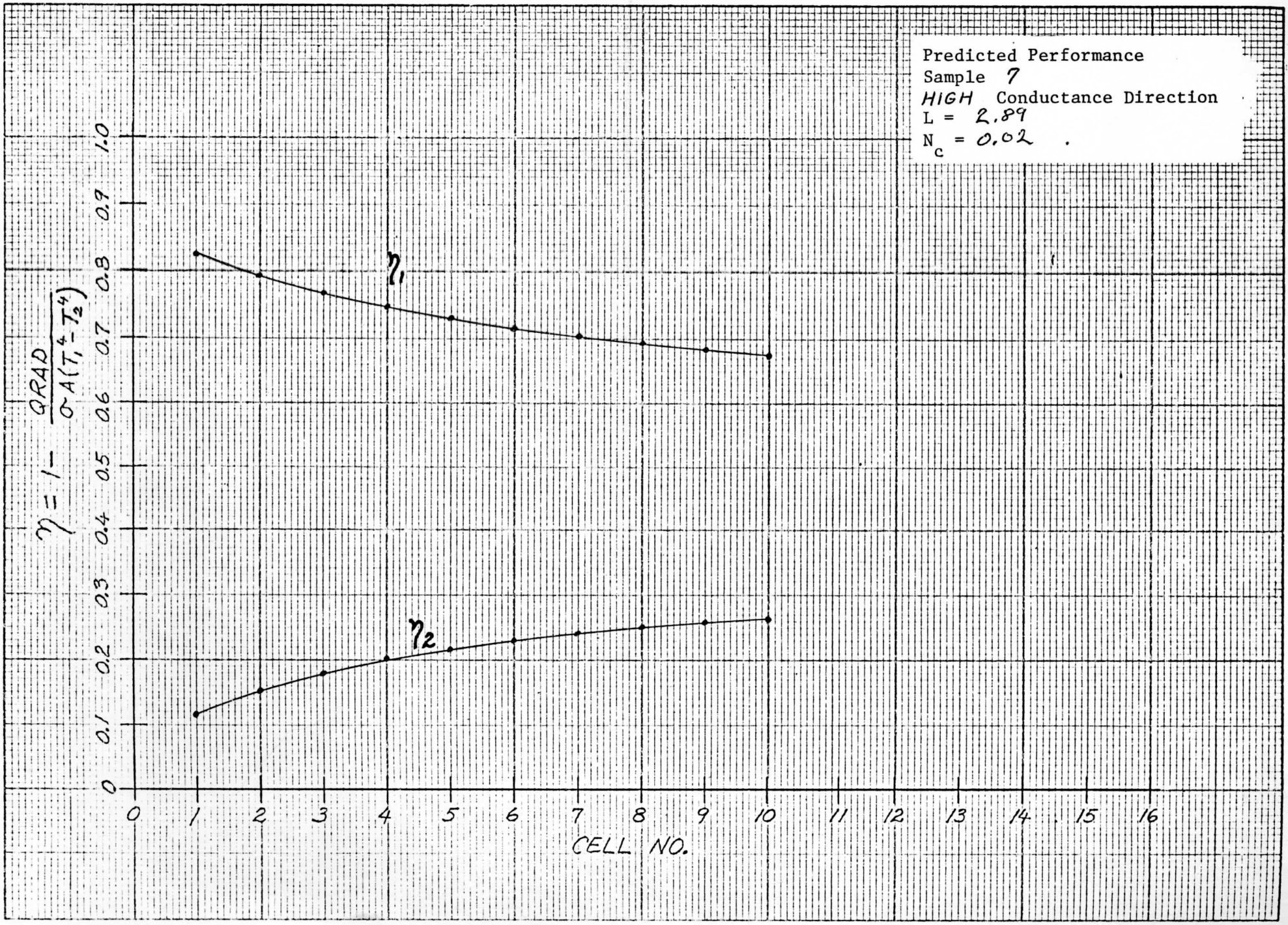
Predicted Performance
Sample 7
HIGH Conductance Direction
L = 2.89
N_c = 0.02
$\eta = 1 - \frac{QRAD}{\sigma A(T_1^4 - T_2^4)}$
η_1
η_2
0
0.1
0.2
0.3
0.4
0.5
0.6
0.7
0.8
0.9
1.0
0
1
2
3
4
5
6
7
8
9
10
11
12
13
14
15
16
CELL NO.

Figure 18

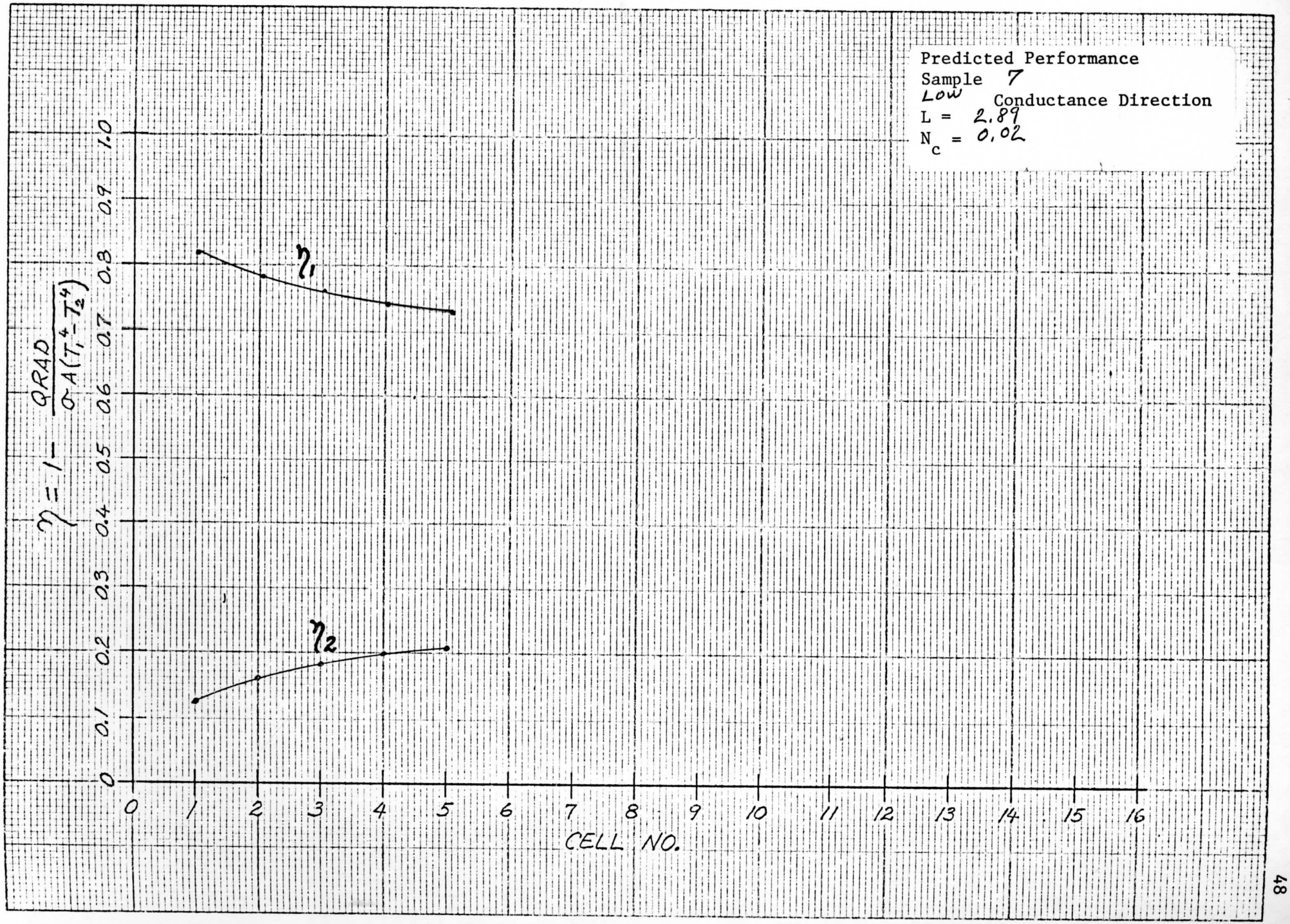
Predicted Performance
Sample 7
Low Conductance Direction
L = 2.89
N_c = 0.02
$\eta = 1 - \frac{Q_{RAD}}{\sigma A(T_1^4 - T_2^4)}$
η_1
η_2
0
0.1
0.2
0.3
0.4
0.5
0.6
0.7
0.8
0.9
1.0
0
1
2
3
4
5
6
7
8
9
10
11
12
13
14
15
16
CELL NO.

Figure 19

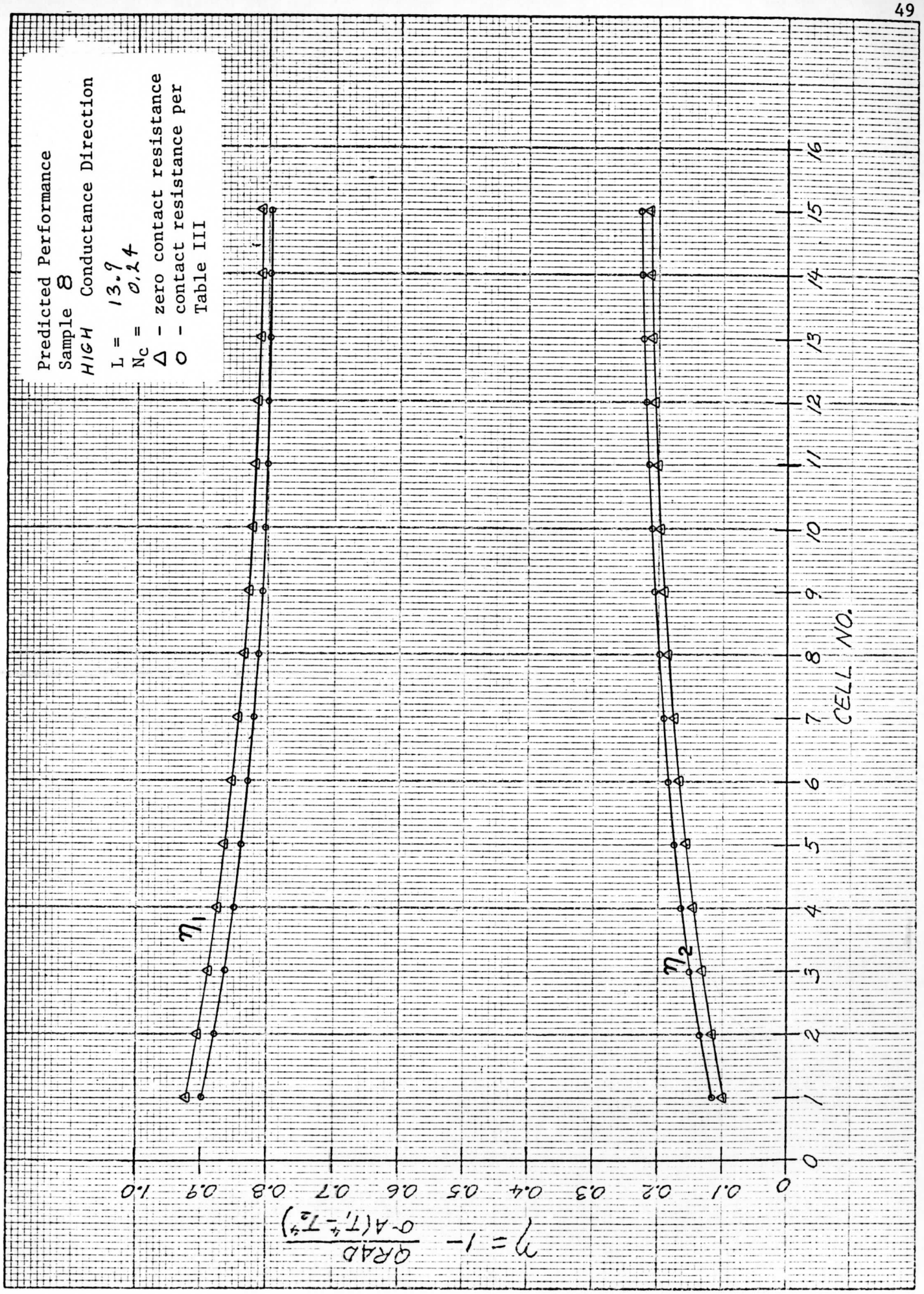
Predicted Performance
Sample 8
HIGH Conductance Direction
L = 13.9
N_c = 0.24
Δ - zero contact resistance
o - contact resistance per Table III
$\eta = 1 - \frac{QRAD}{\sigma A(T_1^4 - T_2^4)}$
η_1
η_2
CELL NO.
0
1
2
3
4
5
6
7
8
9
10
11
12
13
14
15
16
0.1
0.2
0.3
0.4
0.5
0.6
0.7
0.8
0.9
1.0

Figure 20

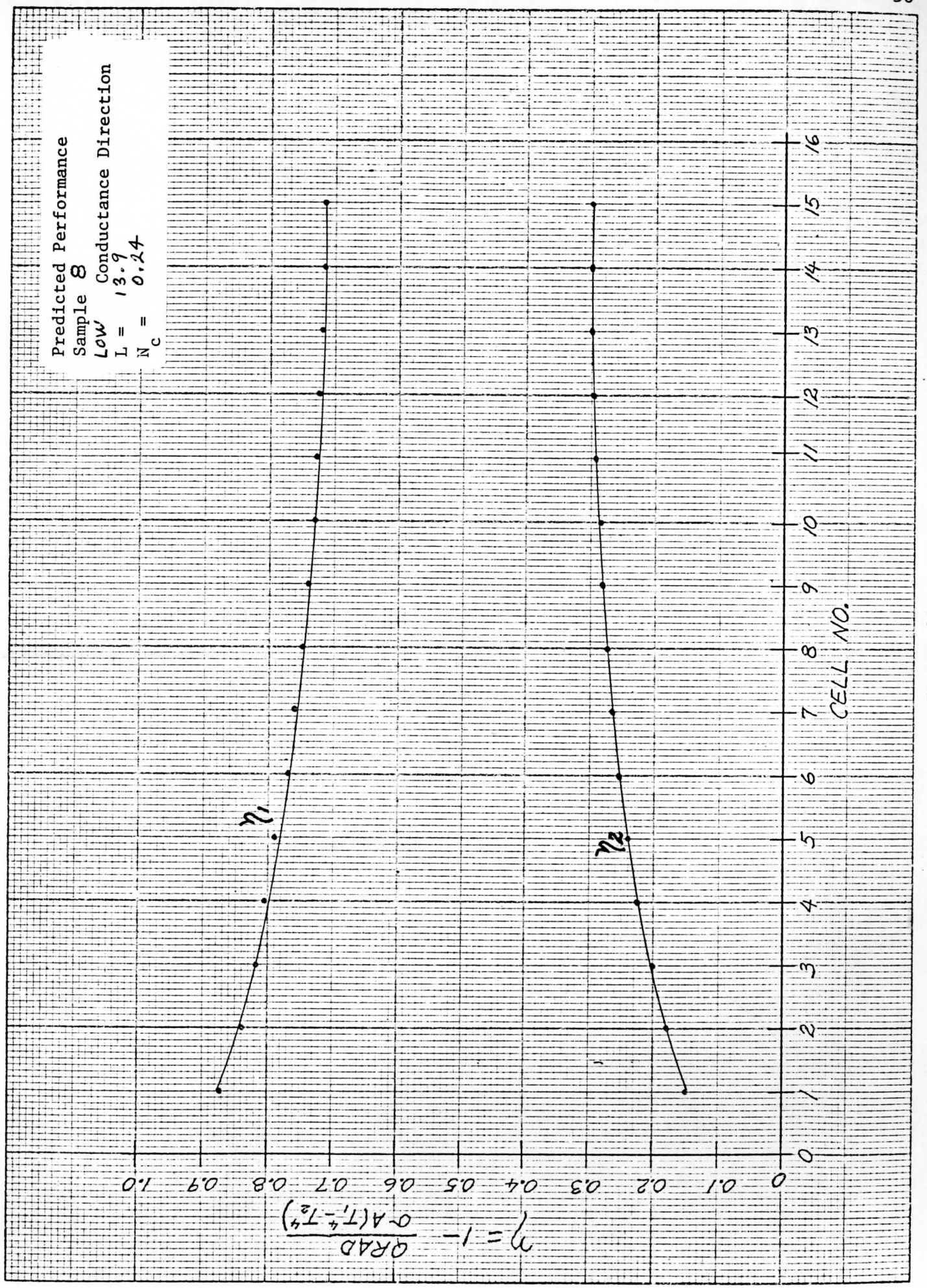
Predicted Performance
Sample 8
Low Conductance Direction
L = 13.9
N_c = 0.24
$\eta = 1 - \frac{QRAD}{\sigma A(T_1^4 - T_2^4)}$
0 0.1 0.2 0.3 0.4 0.5 0.6 0.7 0.8 0.9 1.0
0 1 2 3 4 5 6 7 8 9 10 11 12 13 14 15 16
CELL NO.
η_1
η_2

Figure 21

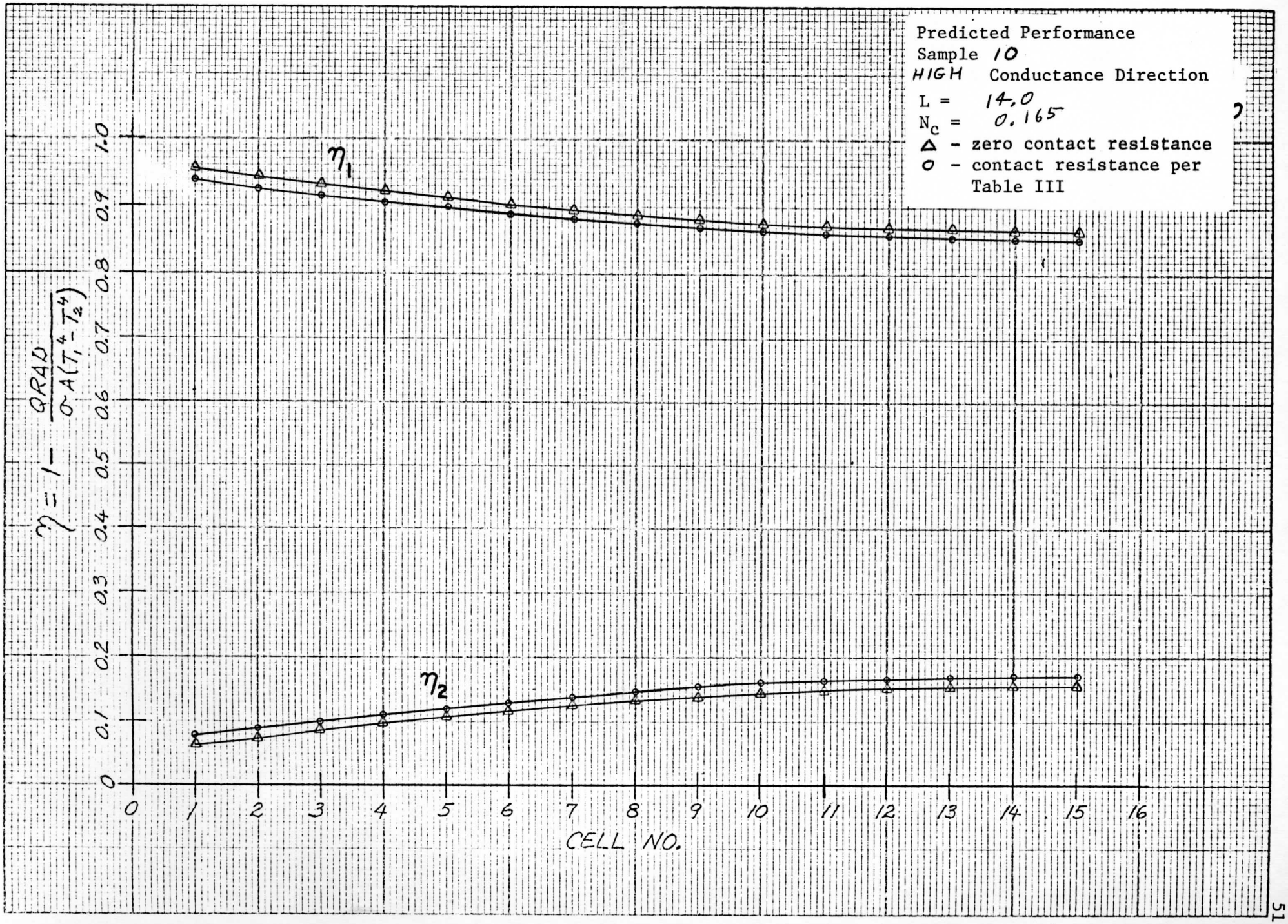
Predicted Performance
Sample 10
HIGH Conductance Direction
L = 14.0
N_C = 0.165
△ - zero contact resistance
○ - contact resistance per Table III
$\eta = 1 - \frac{QRAD}{\sigma A(T_1^4 - T_2^4)}$
η_1
η_2
0
0.1
0.2
0.3
0.4
0.5
0.6
0.7
0.8
0.9
1.0
0
1
2
3
4
5
6
7
8
9
10
11
12
13
14
15
16
CELL NO.

Figure 22

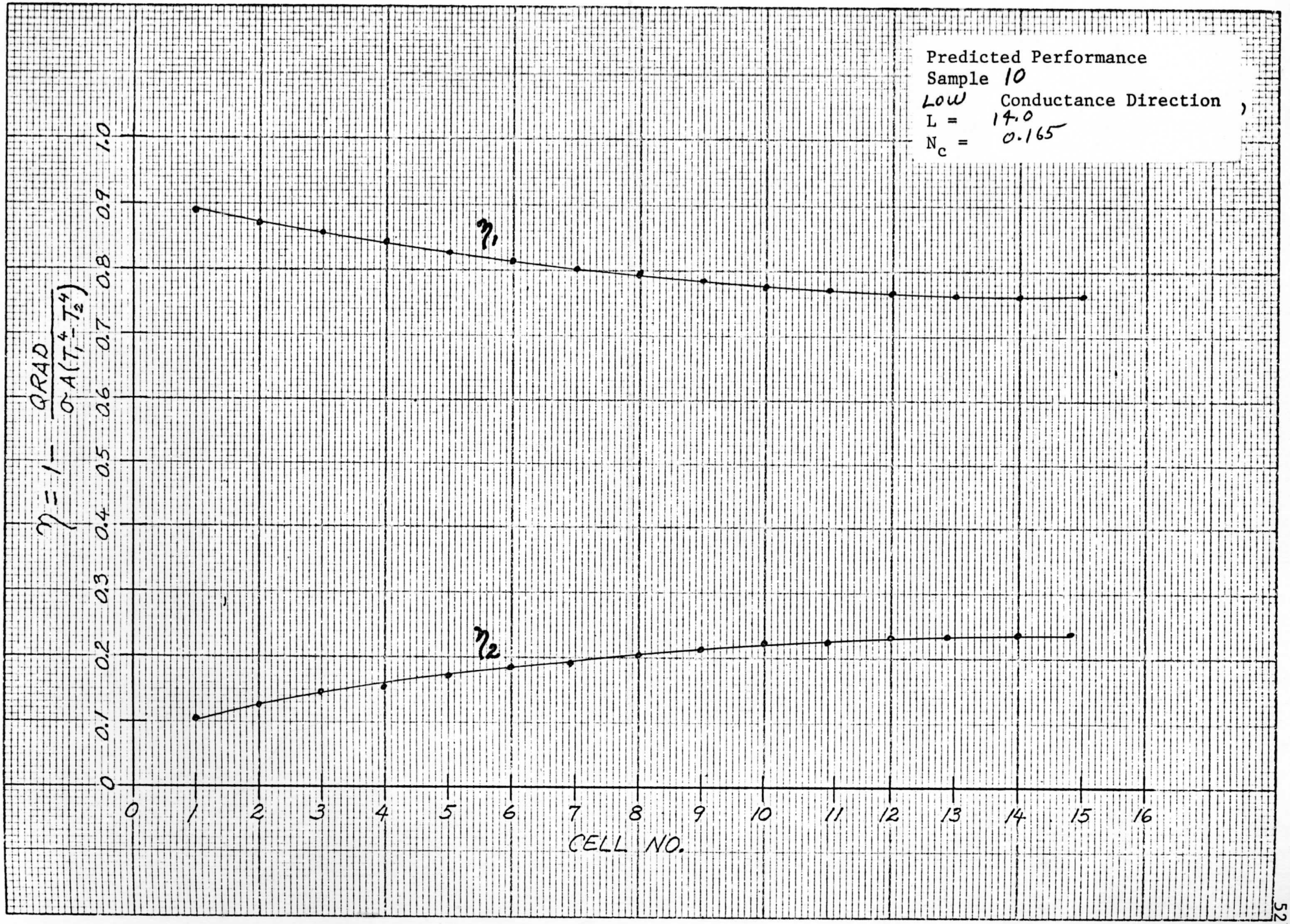
Predicted Performance
Sample 10
Low Conductance Direction
L = 14.0
N_c = 0.165
$\eta = 1 - \frac{QRAD}{\sigma A(T_1^4 - T_2^4)}$
η_1
η_2
0
0.1
0.2
0.3
0.4
0.5
0.6
0.7
0.8
0.9
1.0
0
1
2
3
4
5
6
7
8
9
10
11
12
13
14
15
16
CELL NO.

Figure 23

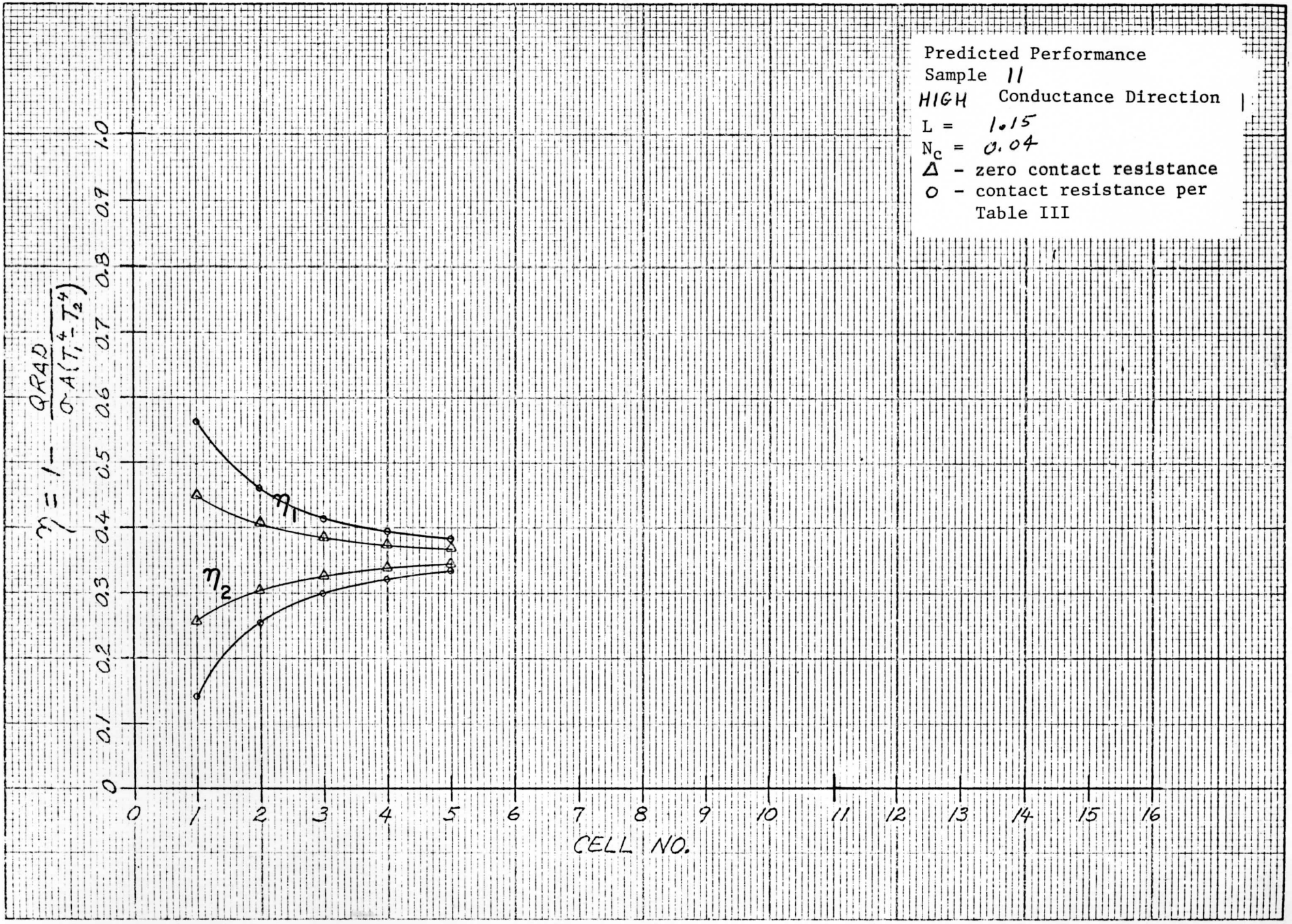
Predicted Performance
Sample 11
HIGH Conductance Direction
L = 1.15
N_c = 0.04
Δ - zero contact resistance
O - contact resistance per Table III
$\eta = 1 - \frac{Q_{RAD}}{\sigma A(T_1^4 - T_2^4)}$
η_1
η_2
0
0.1
0.2
0.3
0.4
0.5
0.6
0.7
0.8
0.9
1.0
0 1 2 3 4 5 6 7 8 9 10 11 12 13 14 15 16
CELL NO.

Figure 24

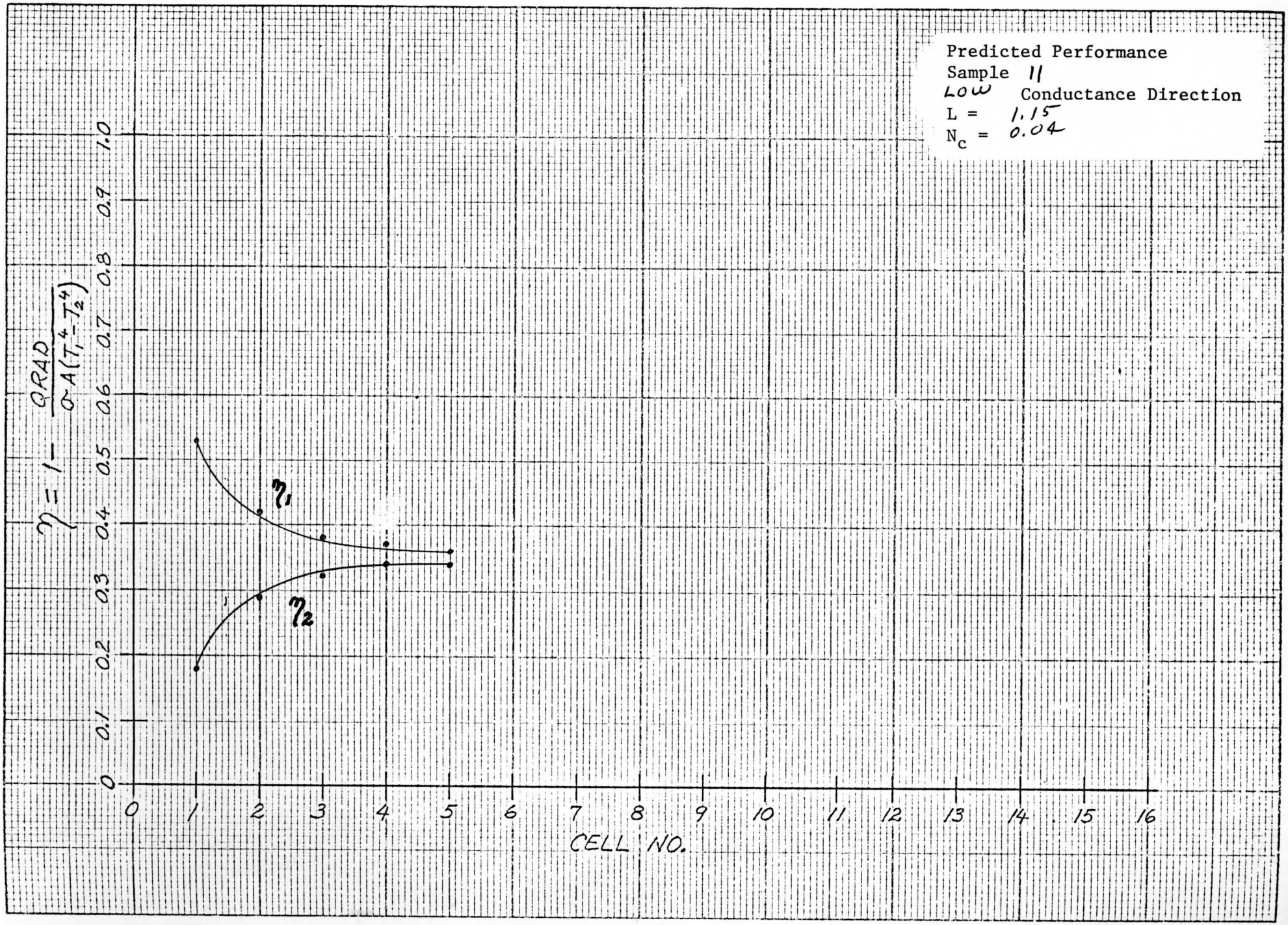
Predicted Performance
Sample 11
Low Conductance Direction
L = 1.15
N_c = 0.04
$\eta = 1 - \frac{QRAD}{\sigma A(T_1^4 - T_2^4)}$
η_1
η_2
0
0.1
0.2
0.3
0.4
0.5
0.6
0.7
0.8
0.9
1.0
0
1
2
3
4
5
6
7
8
9
10
11
12
13
14
15
16
CELL NO.

Figure 25

DIRECTIONAL SPECTRAL REFLECTANCE

CUSTOMER CODE NO.: 3M

TRW DESIGNATION: 123-75

MATERIAL:

ANGLES

POLAR, θ = 15°

AZIMUTHAL, φ = Arbitrary

MEASUREMENT Spectral Reflectance

INSTRUMENTS Edwards-type Integrating Sphere, and Heated Cavity Reflectometer

Total Hemispherical Emissivity = 0.86

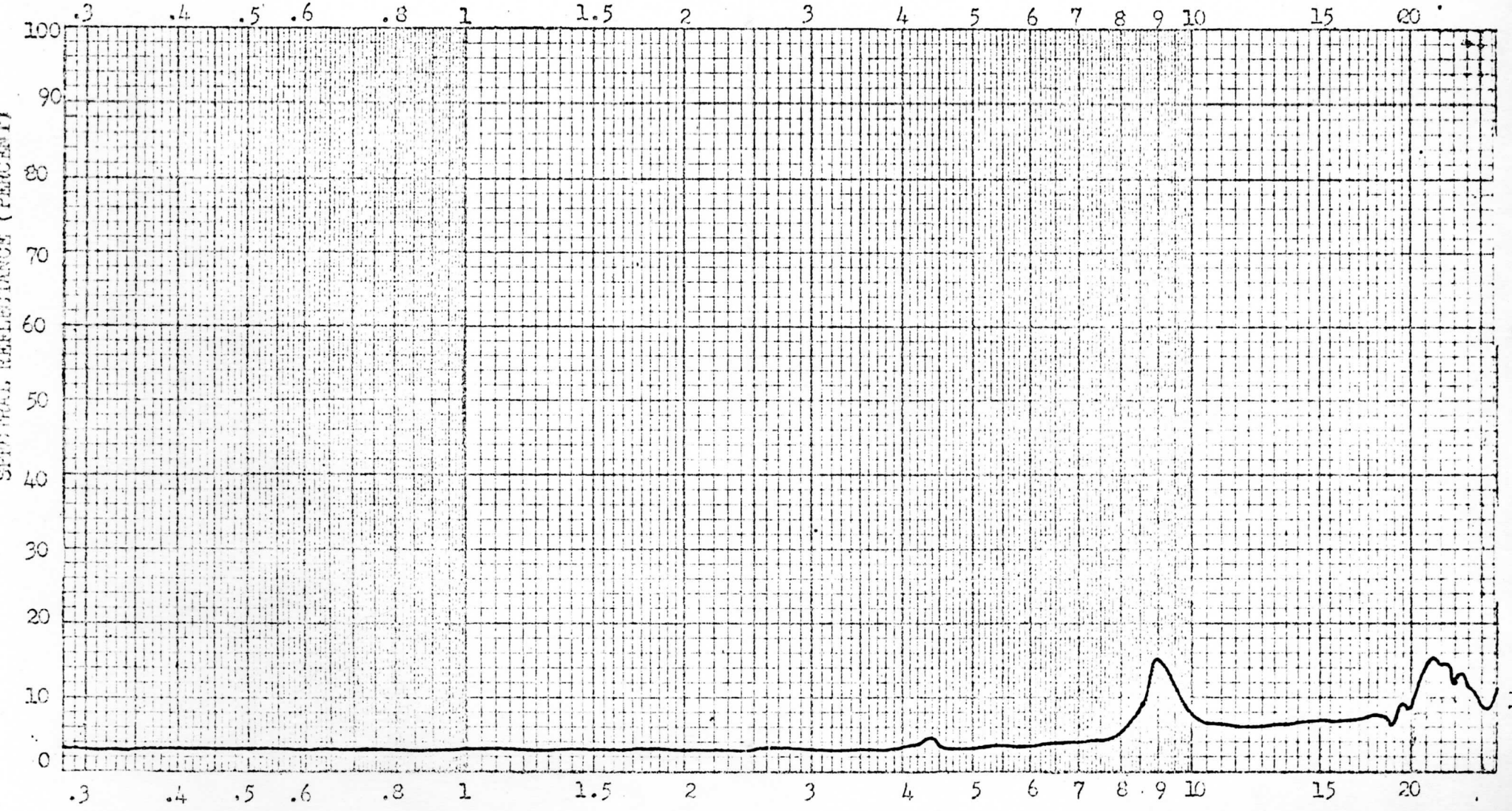

Figure 26

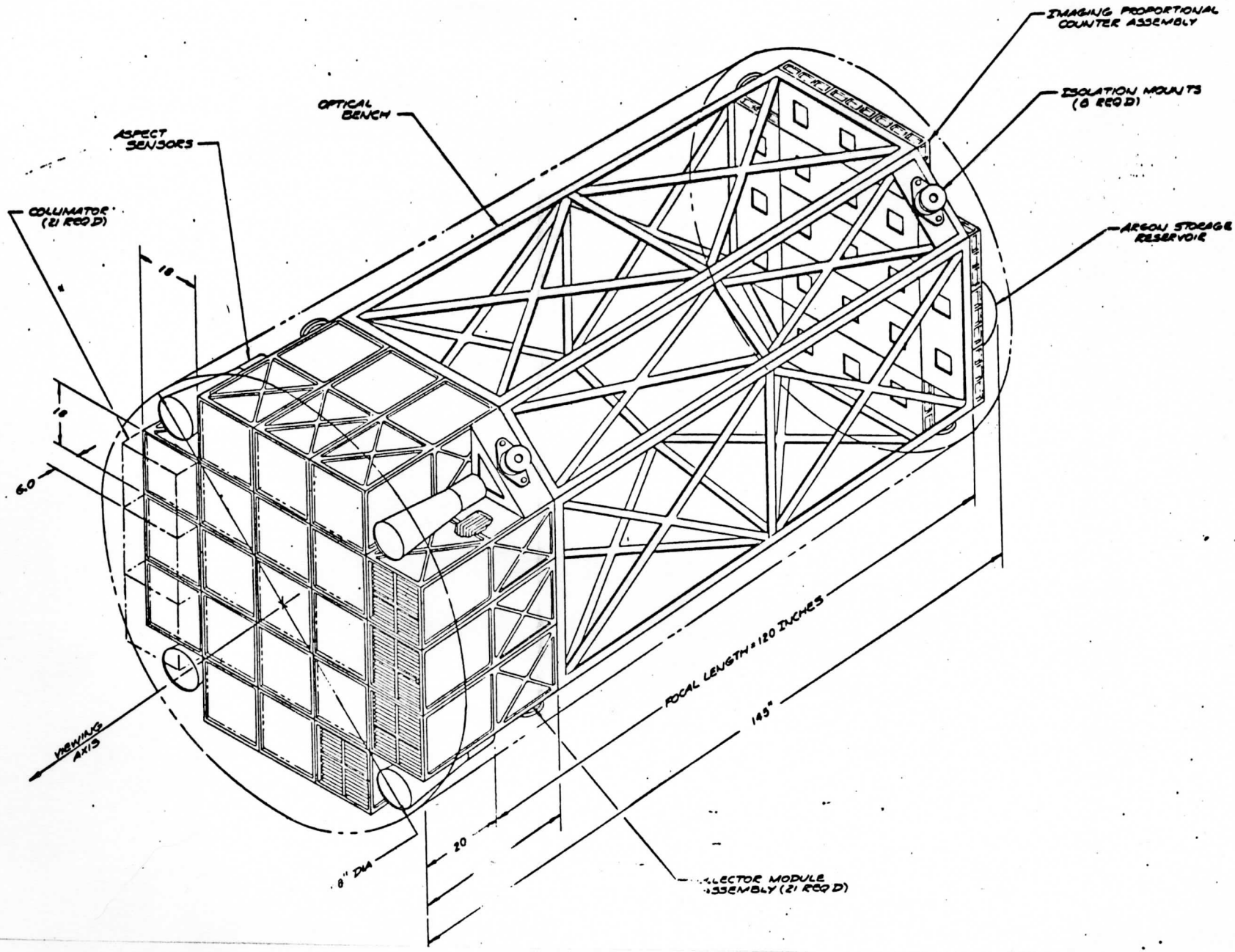

Figure 27. Front view of 21 module LAMAR for large spacecraft. This particular device was made for circular aperture. Mirror assemblies, aspect sensors, insolation mounts and front of detectors can be seen. A 6" deep collimator in front of each module is indicated.

APPENDIX C

CLEAR VIEW CALCULATION

The equivalent field of view of a detector shielded by a Honeycomb Thermal Shield can be approximated by:

$$\Omega_{eqv} = \Omega_{detector} - \frac{\pi}{6} \frac{\theta_D^3}{\theta_s}$$

where:

$$\Omega_{detector} = \pi\left(\frac{W}{g + H}\right)^2 = \text{solid angle in steradians}$$

$$g = [W^2 + H^2]^{1/2}$$

$$\theta_D = \tan^{-1}\left(\frac{W}{H}\right) \text{ for the detector collimator}$$

$$\theta_s = \tan^{-1}\left(\frac{W}{H}\right) \text{ for the Honeycomb Thermal Shield}$$